Department of Energy
Savannah River Operations Office
P.O. Box A
Aiken, South Carolina 29802

JAN 08 2026

Ms. Susan B. Fulmer, P. G., Manager
Federal Remediation Section
Division of Site Assessment, Remediation and Revitalization
Bureau of Land and Waste Management
South Carolina Department of Environmental Services
2600 Bull Street
Columbia, South Carolina 29201

Mr. Jon Richards
Savannah River Site Remedial Project Manager
Superfund and Emergency Management Division
U. S. Environmental Protection Agency, Region 4
61 Forsyth Street, SW
Atlanta, Georgia 30303

Dear Ms. Fulmer and Mr. Richards:

SUBJECT: Scoping Summary for the D-Area Groundwater Operable Unit (U) (Post-Characterization Scoping Phase) (ERD-EN-2019-0022, November 2025) (Final), DAG OU Post-Characterization Scoping Summary/Second Work Plan Addendum Meeting Presentation (SRNS-MS-2025-00564, November 2025) and Supporting Documents, SEMS Number: 63

The U. S. Department of Energy is submitting the information listed below in accordance with the discussions and agreements reached at the November 13, 2025, DAG OU Post-Characterization Scoping Summary Meeting for your files.

- Scoping Summary for the D-Area Groundwater Operable Unit (U) (Post-Characterization Scoping Phase) (ERD-EN-2019-0022, November 2025) (Final),
- DAG OU Post-Characterization Scoping Summary/Second Work Plan Addendum Meeting Presentation (SRNS-MS-2025-00564, November 2025), and
- Journal articles: *Longevity of colloidal activated carbon for in situ pfas remediation at afff-contaminated airport sites* and *Evaluating the longevity of a PFAS in situ colloidal activated carbon remedy*

The time and effort that the South Carolina Department of Environmental Services and the U. S. Environmental Protection Agency have given on the subject operable unit are greatly appreciated.

JAN 0 8 2026

Ms. Susan Fulmer
Mr. Jon Richards 2

Comments or questions from you or your staff may be directed to me at (803) 522-6427.

Sincerely,

MATTHEW BAKER Digitally signed by MATTHEW BAKER Date: 2026.01.08 08:21:08 -05'00'

Matthew R. Baker
Acting FFA Remedial Project Manager
DOE-Savannah River Operations Office
Remediation, Deactivation, and Decommissioning Division

RDDD-26-114

Enclosures:
1. Scoping Summary for the D-Area Groundwater Operable Unit (U) (Post-Characterization Scoping Phase) (ERD-EN-2019-0022, November 2025) (Final) SEMS Number: 63
2. DAG OU Post-Characterization Scoping Summary/Second Work Plan Addendum Meeting Presentation (SRNS-MS-2025-00564, November 2025)
3. Carey, G. R., Hakimabadi, S. G., Singh, M., McGregor, R., Woodfield, C., Van Geel, P. J., & Pham, A. L. (2022). *Longevity of colloidal activated carbon for in situ pfas remediation at afff-contaminated airport sites.* Remediation Journal, 33(1), 3–23. https://doi.org/10.1002/rem.21741
4. Carey, G. R., McGregor, R., Pham, A. L.-T., Sleep, B., & Hakimabadi, S. G. (2019). *Evaluating the longevity of a PFAS in situ colloidal activated carbon remedy.* Remediation Journal, 29(2), 17–31. https://doi.org/10.1002/rem.21593

cc w/o encl:
M. Reece, SCDES-Columbia
H. J. Porter, SCDES-Columbia
J. Blalock, SCDES-Columbia
S. French, SCDES-Columbia
R. G. Stewart, SCDES-Columbia
M. Mehta, SCDES-Columbia
G. O'Quinn, SCDES-Midlands Aiken Environmental Affairs Office
T. G. Corley, SCDES-Midlands Aiken Environmental Affairs Office
C. L. Robertson, SCDES-Midlands Aiken Environmental Affairs Office
E. G. Downing, SCDES-Midlands Aiken Environmental Affairs Office
H. L. Herlong, SCDES-Midlands Aiken Environmental Affairs Office

cc w/encl:
H. H. Cathcart, SCDES-Columbia
B. Martin, EPA-Atlanta
M. McRae, TechLaw, Inc.

ARF-025259
RDDD-26-114

DOI: 10.1002/rem.21593

RESEARCH ARTICLE

WILEY

Evaluating the longevity of a PFAS *in situ* colloidal activated carbon remedy

Grant R. Carey[1] | **Rick McGregor**[2] | **Anh Le-Tuan Pham**[3] | **Brent Sleep**[4] | **Seyfollah Gilak Hakimabadi**[3]

[1]Porewater Solutions, Ottawa, Ontario, Canada

[2]In Situ Remediation Services Ltd., St. George, Ontario, Canada

[3]University of Waterloo, Waterloo, Ontario, Canada

[4]University of Toronto, Toronto, Ontario, Canada

Correspondence
Grant R. Carey, Porewater Solutions, 27 Kingsford Cresent, Ottawa, Ontario K2K 1T5, Canada.
Email: gcarey@porewater.com

Abstract

The remediation of per- and polyfluoroalkyl substances by injection of colloidal activated carbon (CAC) at a contaminated site in Central Canada was evaluated using various visualization and modeling methods. Radial diagrams were used to illustrate spatial and temporal trends in perfluoroalkyl acid (PFAA) concentrations, as well as various redox indicators. To assess the CAC adsorption capacity for perfluorooctane sulfonate (PFOS), laboratory Freundlich isotherms were derived for PFOS mixed with CAC in two solutions: (1) PFOS in a pH 7.5 synthetic water that was buffered by 1 millimolar $NaHCO_3$ (K_f = 142,800 mg^{1-a} L^a/kg and a = 0.59); and (2) a groundwater sample (pH = 7.4) containing PFOS among other PFAS from a former fire-training area in the United States (K_f = 4,900 mg^{1-a} L^a/kg and a = 0.24). A mass balance approach was derived to facilitate the numerical modeling of mass redistribution after CAC injection, when mass transitions from a two-phase system (aqueous and sorbed to organic matter) to a three-phase system that also includes mass sorbed to CAC. An equilibrium mixing model of mass accumulation over time was developed using a finite-difference solution and was verified by intermodel comparison for prediction of CAC longevity in the center of a source area. A three-dimensional reactive transport model (ISR-MT3DMS) was used to indicate that the CAC remedy implemented at the site is likely to be effective for PFOS remediation for decades. Model results are used to recommend remedial design and monitoring alternatives that account for the uncertainty in long-term performance predictions.

1 | INTRODUCTION

Per- and polyfluoroalkyl substances (PFAS) are emerging contaminants that are widespread in the environment and are generally persistent (Hatton, Holton, & DiGuiseppi, 2018). Perfluoroalkyl acids (PFAAs) are the main types of PFAS that are analyzed in soil and groundwater at contaminated sites and generally have low regulatory advisory or cleanup levels. Some PFAS precursors are known to undergo aerobic biodegradation (e.g., Avendano & Liu, 2016; Harding-Marjanovic et al., 2015), where transformation products may include PFAAs. PFAAs have not been observed to undergo biological or abiotic transformation reactions, resulting in persistent plumes at many sites (Hatton et al., 2018).

There are two classes of PFAAs: perfluoroalkyl carboxylates (PFCAs) and perfluoroalkyl sulfonates (PFSAs). The most commonly regulated PFAS in the environment are perfluorooctanoate (PFOA), which is a PFCA, and perfluorooctane sulfonate (PFOS), which is a PFSA. Regulatory cleanup criteria for these and other PFAS are undergoing development; at present, the U.S. Environmental Protection Agency (USEPA) has imposed a Lifetime Health Advisory for PFOS and PFOA individually or in combination, of 0.07 microgram per liter (μg/L; USEPA, 2016a, 2016b). Health Canada drinking water screening values for PFOS and PFOA are 0.6 and 0.2 μg/L, respectively (Health Canada, 2018). These low cleanup levels and the persistent nature of PFAAs pose a significant challenge in remediating PFAS sites.

Granular activated carbon (GAC) is effective for *ex situ* treatment of PFAS in groundwater in some cases (McCleaf et al., 2017). GAC has a typical particle size range of 500 to 1,000 μm, and powdered activated carbon (PAC) may have a particle size of 10 to 100 μm. USEPA (2018) presents a summary of the practice of injecting activated carbon *in situ* as a remediation approach for chlorinated solvents and petroleum hydrocarbons. This includes the high-pressure injection of GAC or PAC, which induces fracturing leading to the heterogeneous distribution of GAC and PAC in thin seams or lenses (USEPA, 2018). Another alternative now being employed is the low-pressure injection of colloidal

activated carbon (CAC) with particle sizes of 1 to 2 μm, which does not induce fracturing and results in a more uniform distribution of activated carbon in the target treatment zone (USEPA, 2018). CAC can be readily injected into fine to coarse sand aquifers (grain sizes of 60–70 μm and greater).

In the case of PFAAs, *in situ* CAC injection may be conducted in a grid pattern to reduce the mass flux from a source zone, or CAC may be injected in a permeable barrier to intercept a plume. Previous work with PFAS sorption to GAC indicates that activated carbon has a high sorption capacity for some PFAS (Appleman et al., 2014; McCleaf et al., 2017). Yu, Zhang, Deng, Huang, and Yu (2009) determined that the sorption capacity associated with activated carbon is higher for smaller sized particles of activated carbon (e.g., PAC versus GAC), because the smaller particles have a higher external surface area per mass of activated carbon. PFAS will eventually break through when the adsorption capacity of *in situ* CAC becomes depleted (USEPA, 2018). Models incorporating Freundlich adsorption behavior and a mechanism for redistributing PFAS mass after CAC injection can be used to assess the longevity of a CAC remedy, and the frequency at which additional CAC may need to be injected to prevent breakthrough.

The benefits of a radial diagram visualization method for assessing the distribution of numerous PFSAs and PFCAs in monitoring wells are demonstrated.

McGregor (2018) presented a case study in which PFOS and PFOA were successfully immobilized through *in situ* injection of CAC at a site in Central Canada. The current study develops a numerical model to evaluate the longevity of this *in situ* remediation approach for this site. The benefits of a radial diagram visualization method for assessing the distribution of numerous PFSAs and PFCAs in monitoring wells are demonstrated. PFOS-CAC isotherms are presented based on laboratory experiments involving a pH 7.5 synthetic solution containing only PFOS and 1 millimolar (mM) $NaHCO_3$ (which serves as a pH buffer; 1 mM HCO_3^- is also a typical alkalinity of groundwater), and a PFAS mixture in a groundwater sample (pH 7.4) collected at a former fire-training area in the United States. A mass balance is incorporated into a numerical model to simulate the redistribution of mass from the original two-phase system (aqueous and sorbed to soil organic matter), to the three-phase system after CAC injection (including sorption to CAC attached to sand grains). An equilibrium mixing model (EMM) is developed for estimating CAC longevity in the middle of a source zone. A sensitivity analysis is conducted to evaluate the range in longevity from a single CAC injection based on isotherm parameters and the fraction of CAC retained in the injection zone.

2 | STUDY SITE

The implementation of the *in situ* CAC remedy at the study site in Central Canada is summarized by McGregor (2018). Occasional fire-training activities at the site resulted in a low-level PFAS plume at the site, with preremedy concentrations of PFOS and PFOA up to approximately 1.5 and 3.3 μg/L, respectively. There were also localized sources of petroleum hydrocarbons in different portions of the site due to other activities. The shallow overburden aquifer at the site is composed of medium sand with some silt. The vertical interval impacted by PFAS at the site occurred over a depth of 0.9 to 1.7 meters (m) below ground surface. The average hydraulic conductivity was 2.6 meters per day (m/d), and the average horizontal hydraulic gradient was 0.06 m/m. Based on an effective porosity of 0.2 m^3/m^3, the average linear groundwater velocity was 0.8 m/d.

The *in situ* remediation approach involved the low-pressure injection of CAC and an oxygen-releasing material into the shallow overburden aquifer. Fifty temporary injection wells were used in total at the site with a grid spacing of approximately 3 m, although only about half of those wells were needed in the vicinity of the PFAS source. Proprietary additives including an organic polymer are included in the CAC solution to stabilize CAC and to facilitate transport in the subsurface. The injection event was conducted over a two-day period in spring 2016 at a cost of less than CAD$100,000.

McGregor (2018) indicates that CAC was observed at a distance up to 4.6 m from an injection point based on soil samples collected at multiple locations and depth intervals 19 months after the injection event. The average fraction of CAC (f_{cac}) measured in the target zone after injection was approximately 0.02% (i.e., 0.23 grams per kilogram) with a maximum measured concentration of 0.04%. The fraction of organic carbon (f_{oc}) was measured to be 0.001% outside the target treatment zone.

Exhibit 1 shows the location of the suspected PFAS source area, the extent of the CAC zone postinjection in the vicinity of this PFAS source zone, and charts of PFOS concentration versus time at monitoring wells with available data (MW-1, MW-2, MW-5, and MW-8). The PFAS source area has an average length of 6.5 m, width of 4.5 m, and an area of 30 m^2. The CAC zone shown in Exhibit 1 extends 10 m downgradient of the PFAS source area. This creates a CAC buffer downgradient of the source area, which helps to increase the remedy longevity, as discussed further below. The extent of the CAC zone was approximated by delineating an area that extended approximately 3 m outside the grid of temporary injection wells. (The northern extent of the CAC zone that was used to remediate only petroleum hydrocarbons is not shown in Exhibit 1.)

The charts shown in Exhibit 1 illustrate that the concentration of PFOS in groundwater was reduced by orders of magnitude (below the detection limit of 0.03 μg/L) after the CAC injection. There was only one detection of PFOS at 0.04 μg/L approximately 1.5 years after the CAC injection event, although PFOS was not detected in a subsequent monitoring round conducted approximately 2 years after the injection event. The source of PFOS detected at one well in this single monitoring event is uncertain and may be due to cross-contamination in the field or in the laboratory.

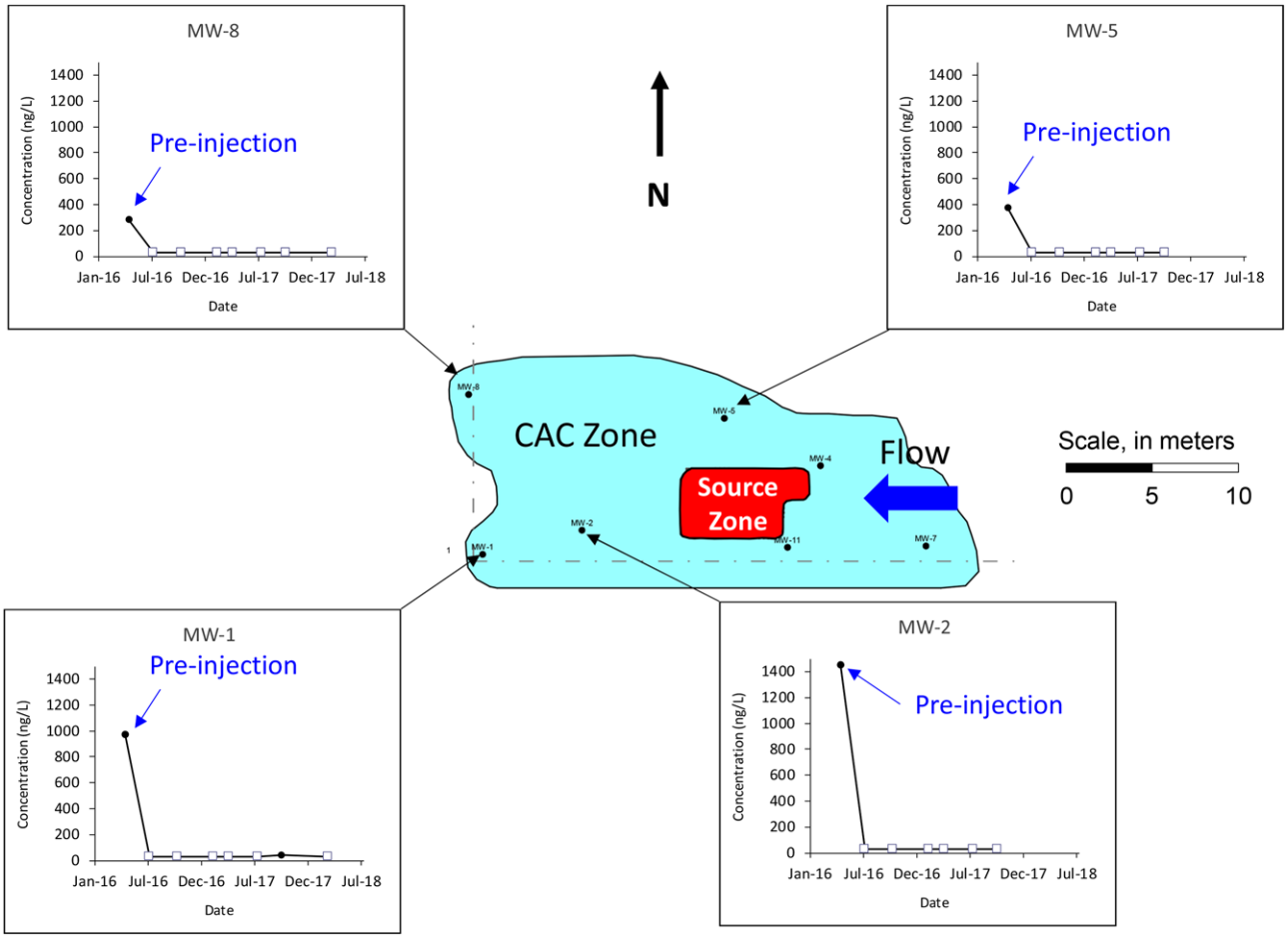

EXHIBIT 1 PFOS concentrations versus time charts (Note that the CAC injection event was in spring 2016)

2.1 | Radial diagram visualization

Carey et al. (1999, 2003) discussed how radial diagrams may be effective for evaluating both spatial and temporal trends for petroleum hydrocarbons, chlorinated solvents, and/or reduction-oxidation (redox) indicators. Given the multispecies nature of PFAS mixtures at many sites, radial diagrams may also be effective for visualizing trends for PFAS at contaminated sites.

During initial monitoring events at the site, only PFOS and PFOA were analyzed. In October 2017, a suite of PFAAs were analyzed to see if other PFAS constituents were detectable in groundwater after the CAC injection event. Exhibit 2 presents radial diagrams representing nine PFCAs that were analyzed in October 2017, including perfluorobutanoate (PFBA), perfluoropentanoate (PFPeA), perfluorohexanoate (PFHxA), perfluoroheptanoate (PFHpA), PFOA, perfluorononanoate (PFNA), perfluorodecanoate (PFDA), perfluoroundecanoate (PFUnA), and perfluorododecanoate (PFDoA). The legend shown at the top right of Exhibit 2 represents PFCA concentrations at a single monitoring well (MW-1), where each axis of the radial diagram represents the concentration of a single PFCA constituent. The axes of the radial diagram are ordered counterclockwise in the sequence of increasing molecular chain length. The orange-shaded data series represents October 2017 concentrations for each PFCA. A white symbol is used to represent nondetects and is plotted at a concentration equivalent to one-half of the detection limit. A single black symbol is used to show the preinjection PFOA concentration injection (when the other constituents were not analyzed).

Radial diagrams are shown for five monitoring wells at the site in Exhibit 2; four wells within the CAC zone (MW-1, MW-2, MW-5, and MW-8), and one well outside the CAC zone (MW-9) where PFOA was not detected prior to CAC injection. Comparison of the preinjection and October 2017 PFOA concentrations at monitoring wells within the CAC zone indicates that PFOA concentrations were still reduced by at least one order of magnitude 19 months after the injection event. There was only one detection of any PFCA constituent at any of the wells at the site in October 2017 (PFUnA at MW-1 with a concentration of 0.02 μg/L). This is the same well where PFOS was detected at a low concentration in October 2017. Monitoring conducted in March 2018 indicated that all PFAAs were nondetect at MW-1, including PFOS and PFUnA. The cause of these two detections in October 2017 is unknown, although it may be related to cross-contamination during sample collection in the field, or sample handling in the laboratory.

The use of radial diagrams is beneficial when evaluating spatial and temporal trends for a number of PFAS constituents across the site. If preinjection samples had been analyzed for all PFCAs instead of just PFOA, then another series could have been plotted on each radial diagram instead of the single symbol for PFOA. These radial diagrams were plotted using Visual Bio (Porewater Solutions, 2017),

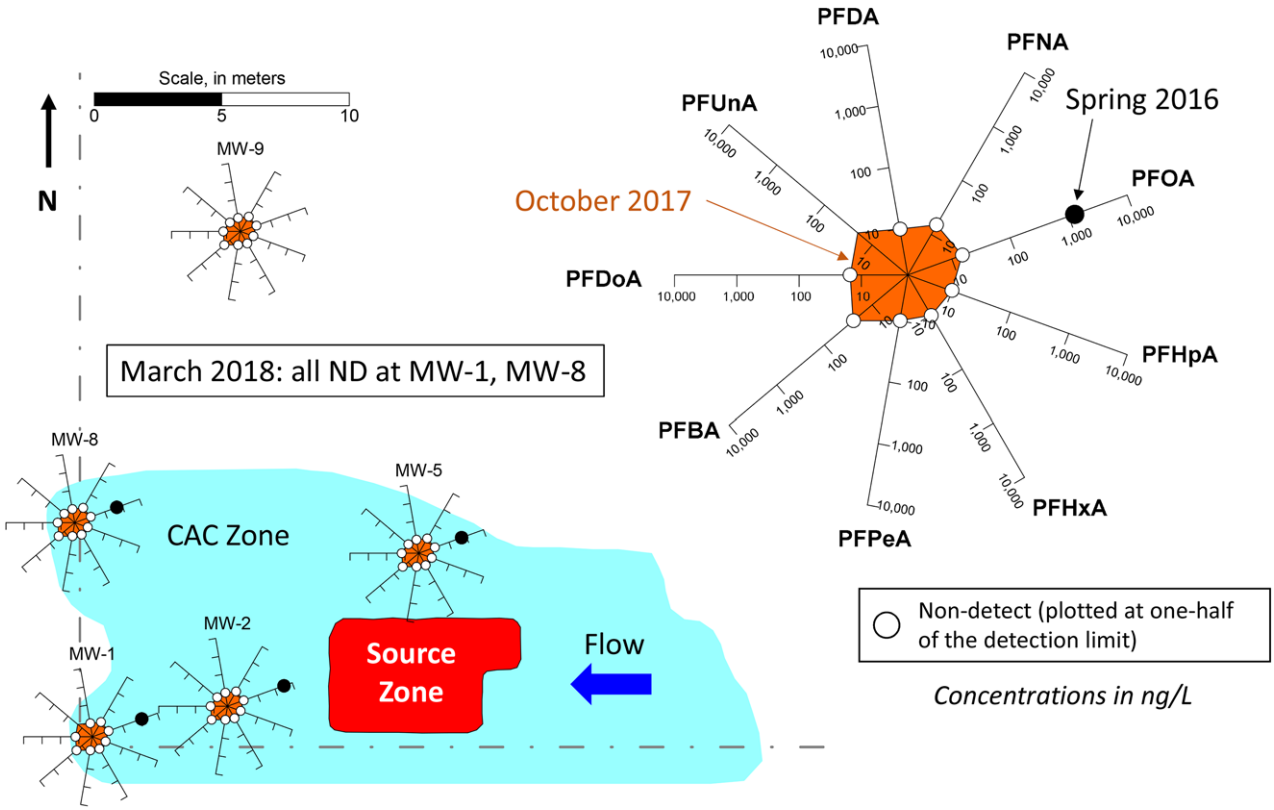

EXHIBIT 2 PFCA radial diagrams (October 2017)

which is available for free download at http://www.porewater.com/visualbio-download.html.

Exhibit 3 presents radial diagrams representing PFSAs that were analyzed in October 2017, including perfluorobutane sulfonate (PFBS), perfluorohexane sulfonate (PFHxS), PFOS, and perfluorodecane sulfonate (PFDS). Analytical results for perfluorooctane sulfonamide (PFOSA), a precursor to PFAAs, are also presented on the radial diagrams shown in Exhibit 3. Similar to Exhibit 2, nondetect symbols are shown in Exhibit 3 as well as a single symbol for PFOS preinjection concentrations (because other PFSAs were not analyzed prior to CAC injection). Exhibit 3 shows that all PFSAs were nondetect at the site except for a low concentration of PFOS detected at MW-1 as discussed above. Monitoring conducted in March 2018 indicated that all PFAAs were nondetect, which suggests that the lone detection of PFOS may be related to cross-contamination.

Exhibits 2 and 3 indicate that the postinjection PFAA concentrations are less than the method detection limits of 0.02 to 0.03 μg/L in the CAC zone, and that they have stayed low for a period of two years. These shorter term monitoring data provide valuable insights that inform on the range of isotherm properties that occurs *in situ* at the site; that is, these results may be used to rule out ranges of isotherm properties that are not realistic for the site. As shown below, these monitoring data may be used to constrain the range of PFOS-CAC isotherm properties that are applicable for evaluating remedy longevity.

Exhibit 4 shows redox radial diagrams representing trends at site wells for four redox indicators (dissolved oxygen, oxidation-reduction potential [ORP], nitrate, and sulfate), for three monitoring events: (1) Spring 2016 prior to CAC injection; (2) April 2017 (13 months after injection); and (3) October 2017 (19 months after injection). The yellow data series represent the redox indicator concentrations corresponding to the respective monitoring event. The size of the yellow data series indicates the extent to which conditions are oxidizing (i.e., aerobic) or reducing (i.e., anaerobic).

Exhibit 4a shows that prior to CAC injection, groundwater upgradient from the PFAS source zone was generally aerobic where the yellow data series are relatively large in extent (MW-4, MW-5, and MW-7). Exhibit 4a also shows that groundwater was generally anaerobic downgradient of the PFAS source zone area prior to CAC injection (MW-1, MW-2, MW-8, and MW-11). The transition from aerobic background to downgradient anaerobic conditions is probably due to the biodegradation of petroleum hydrocarbons that were generally colocated with the PFAS plume that was present prior to CAC injection. Exhibit 4b illustrates that groundwater conditions at downgradient monitoring wells (MW-1, MW-2, and MW-8) had changed from anaerobic conditions prior to the injection event, to aerobic conditions 13 months after the injection event. This change is consistent with the inclusion of oxygen-releasing material in the solution injected in spring 2016, creating sustained aerobic conditions within the injection zone.

Exhibit 4c illustrates that dissolved oxygen and ORP levels declined between April and October 2017, indicating that the oxygen-releasing material was being depleted. As shown in Exhibits 1 through 3, the presence of aerobic conditions did not cause an increase in the concentrations of PFAAs in groundwater due to potential precursor biodegradation. This may be due to low concentrations of precursors being present prior to CAC injection, or that PFAAs that may have been

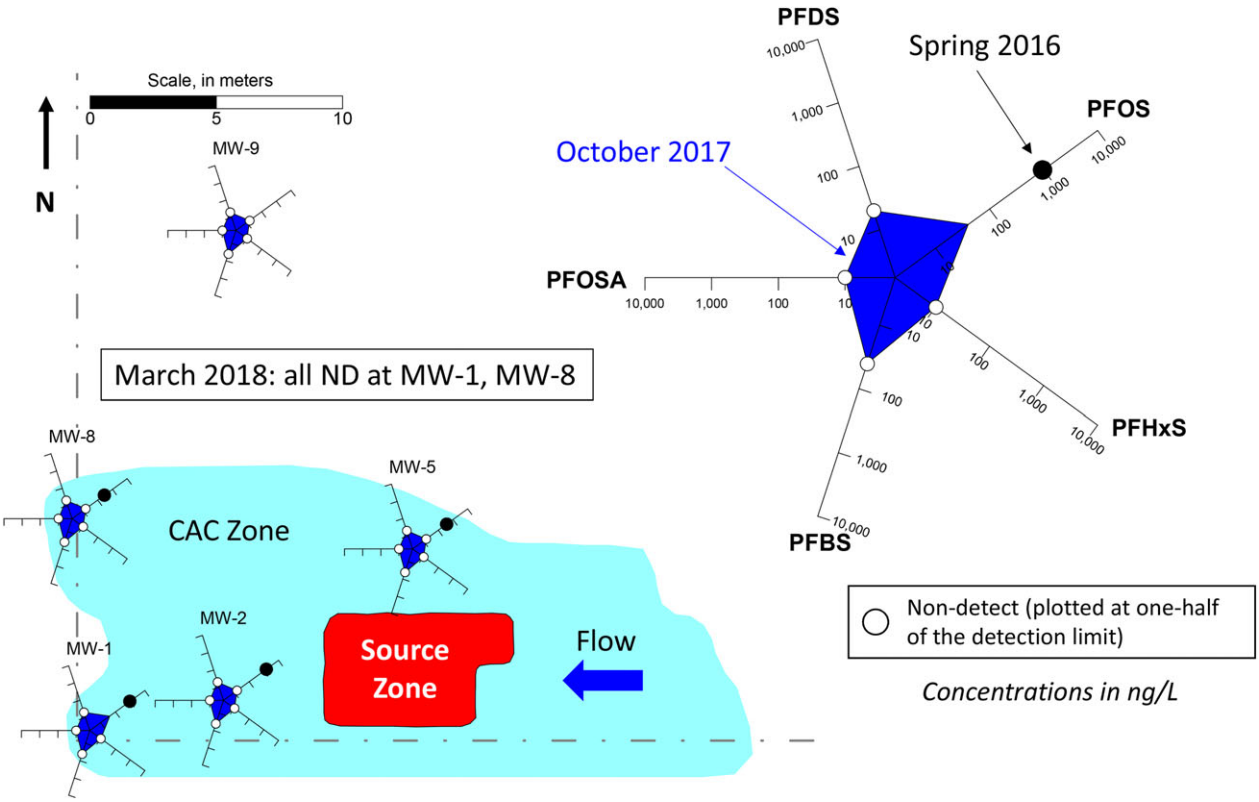

EXHIBIT 3 PFSA radial diagrams (October 2017)

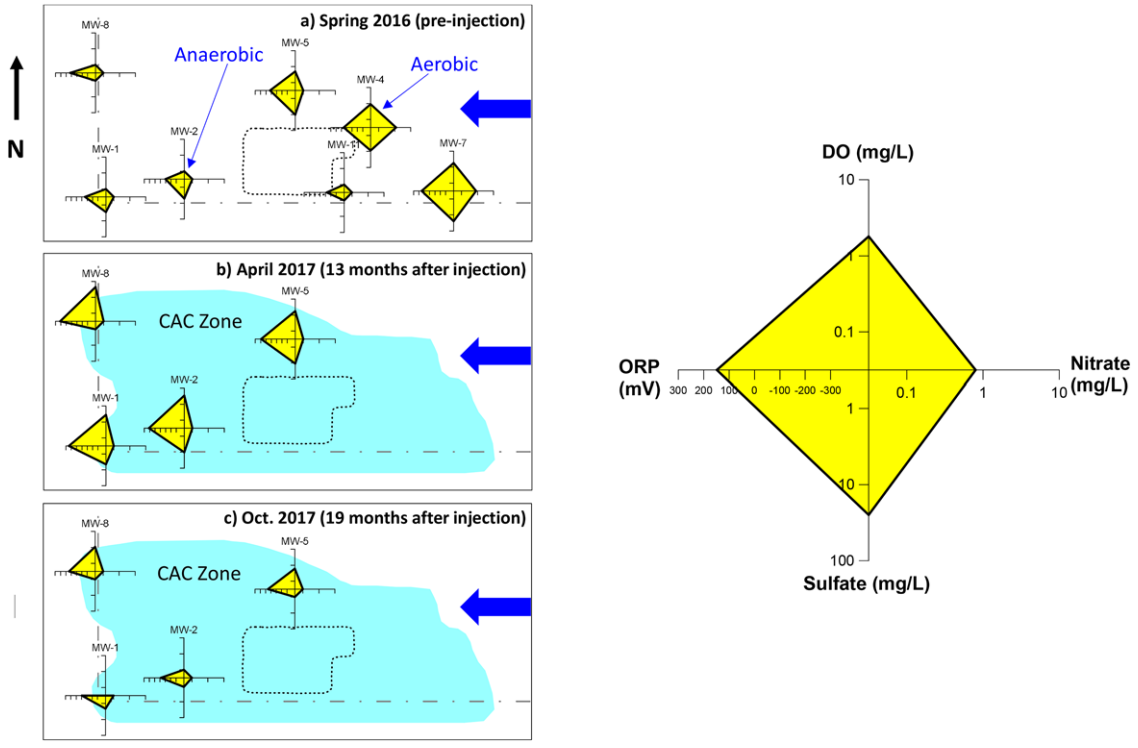

EXHIBIT 4 Redox radial diagrams (October 2017)

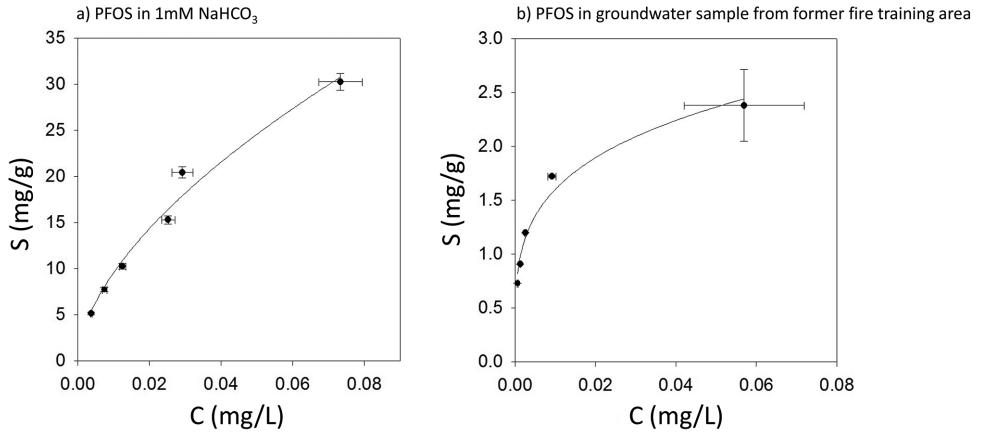

EXHIBIT 5 PFOS-CAC isotherms for a pure solution and a PFAS groundwater sample from a former fire-training area. *S* is the PFOS concentration sorbed to CAC, and *C* is the PFOS aqueous concentration

produced during aerobic biodegradation of precursors were subsequently sorbed to CAC in the soil.

3 | PFOS-CAC ISOTHERMS

PFAS sorption to *in situ*-activated carbon follows Freundlich isotherm behavior, such that the chemical concentration sorbed to CAC in soil is determined based on

$$S_{CAC} = K_f\, f_{cac}\, C^a \quad (1)$$

where S_{CAC} is the contaminant concentration sorbed to CAC in soil (milligrams per kilogram [mg/kg]); K_f is the Freundlich CAC partitioning coefficient (milligrams$^{1\text{-}a}$ liter^a per kilogram mg$^{1\text{-}a}$ L^a/kg); f_{cac} is the fraction of CAC in soil (g/g); *C* is the contaminant aqueous concentration in groundwater (milligrams per liter [mg/L]); and *a* is the Freundlich isotherm exponent (dimensionless).

K_f is sometimes referred to as the sorption capacity for a sorbent and is equal to the soil concentration that occurs in when *C* is 1 mg/L. The Freundlich isotherm exponent *a* reflects the degree of nonlinearity in the isotherm; when $a = 1$, the isotherm simplifies to the linear sorption isotherm.

When the Freundlich isotherm represents the dominant sorption mechanism, a nonlinear retardation coefficient may be estimated using

$$R_{cac} = 1 + \frac{\rho_b}{\theta}(K_f\, f_{cac}\, a\, C^{a-1}) \quad (2)$$

where R_{cac} is the retardation coefficient (dimensionless); θ is effective porosity (L/L); and ρ_b is soil dry bulk density (g/mL).

Equations (1) and (2) demonstrate that the Freundlich isotherm properties (K_f and *a*) and f_{cac} have a significant influence on the PFAS retardation coefficient associated with CAC. A previous study developed a PFOS isotherm with CAC where $K_f = 55{,}890$ mg$^{1\text{-}a}$ L^a/kg and $a = 0.47$ (Regenesis, 2016).

In this study, PFOS-CAC isotherms were determined for (1) pure solution in 1 mM $NaHCO_3$ ($K_f = 142{,}800$ mg$^{1\text{-}a}$ L^a/kg, $a = 0.59$); and (2) PFAS mixture in a groundwater sample collected in the vicinity of a former fire-training area in the United States ($K_f = 4{,}900$ mg$^{1\text{-}a}$ L^a/kg, $a = 0.24$). The groundwater sample with the PFAS mixture had a PFOS concentration of 208 μg/L, and the total detected concentrations of PFSAs, PFCAs, and (mainly fluorotelomer) precursors were 281.8, 46.9, and 60.2 μg/L, respectively. PFAS analytical results for this groundwater sample are presented in Supporting Information Table S1. PFOS, on a mass basis, was approximately 53% of the total detected PFAS in the groundwater sample. The concentration of total organic carbon (TOC) in the groundwater sample from the former fire-training area was 23.8 mg/L.

Each isotherm was determined based on batch experiments performed in triplicate. Exhibit 5 shows the charts of sorbed versus aqueous concentrations determined for these two isotherms. The isotherms were developed by adding different amounts of CAC into solution, and measuring the amount of PFOS that remained in solution (see Supporting Information for detailed information on the experimental procedure). The concentration of PFOS remaining in solution after equilibrating with CAC ranged from 4 to 70 μg/L for the 1 mM $NaHCO_3$ solution isotherm, and from 0.6 to 57 μg/L for the PFAS groundwater sample isotherm.

The difference between these two isotherms may be related to the effects of competitive sorption in the groundwater PFAS sample isotherm, due to the presence of other PFAS, TOC, and/or other co-contaminants. The groundwater sample contained 23.8 mg/L TOC. Differences in these two isotherms may also be related to differences in geochemistry between the two isotherm solutions. The effects of competitive sorption and geochemistry on PFOS-CAC isotherms are not well understood and are currently undergoing further study.

The Freundlich partitioning coefficient (K_f) is approximately 30 times lower for the groundwater sample with the PFAS mixture, relative to the isotherm determined with the PFOS single-component solution. A lower K_f associated with PFAS mixtures will tend to reduce longevity of an *in situ* CAC remedy. In contrast, the groundwater PFAS mixture isotherm has a lower Freundlich exponent (*a*), which will tend

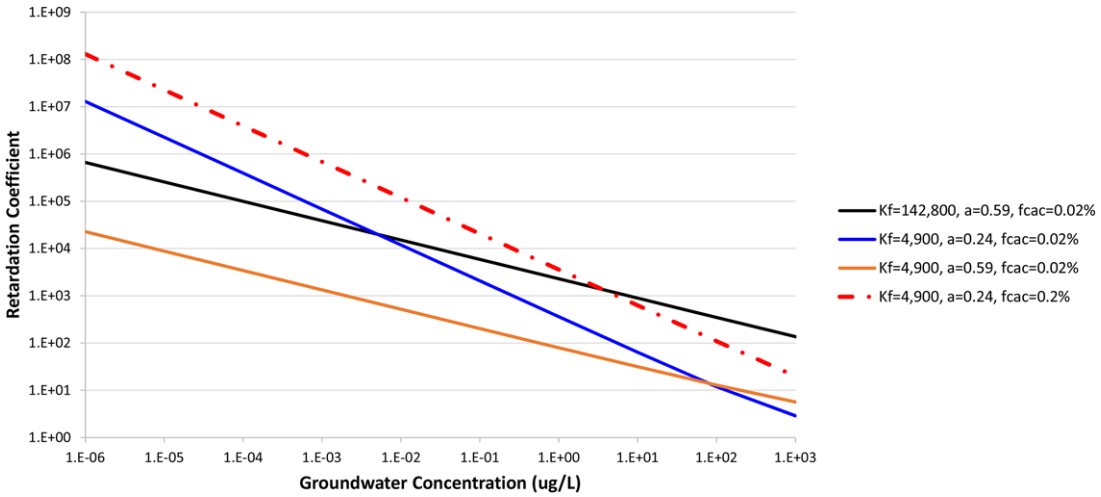

EXHIBIT 6 Retardation coefficient versus aqueous concentration of PFOS within CAC zone. K_f units are mg^{1-a} L^a/kg

to increase the longevity of an *in situ* CAC remedy when PFAS concentrations are low. PFOS-CAC isotherms are likely dependent on site-specific groundwater characteristics, and thus may need to be determined for a given site to reduce uncertainty in CAC performance.

Exhibit 6 plots the retardation coefficient (based on Equation (2)) versus the aqueous concentration of PFOS measured in groundwater after CAC injection and the subsequent mass redistribution step that is discussed further below. When modeling *in situ* CAC performance, the numerical model applies the Freundlich isotherm parameters over a larger range in aqueous concentrations than that which is utilized during the isotherm experiments. This creates uncertainty in the magnitude of the retardation factor at very low aqueous concentrations, which should be considered when evaluating model predictions.

Exhibit 6 demonstrates that, for aqueous concentrations of PFOS below approximately 0.01 μg/L, the retardation coefficient is higher for the isotherm derived from the groundwater that contained a mixture of PFAS (blue solid line) relative to the retardation coefficient associated with the solution containing only PFOS (black solid line). Even though the K_f is approximately 30 times higher for the latter solution, the Freundlich exponent *a* is more than 50% lower for the groundwater sample from the former fire-training area. This demonstrates that a small difference in the Freundlich exponent *a* can have a significant influence on the retardation coefficient.

Exhibit 6 also illustrates that a higher f_{cac} in soil will result in a proportional increase in the retardation coefficient (e.g., when f_{cac} is increased from 0.02% to 0.2%), which is also indicated by Equation (2). This indicates that the remedy performance in the long term may be engineered or improved by injecting higher concentrations of CAC.

4 | MODEL DEVELOPMENT

Prior to CAC injection, contaminant mass will be present in at least two phases (ignoring the potential for nonaqueous phase liquid): The aqueous phase (i.e., dissolved in groundwater) and sorbed to naturally occurring organic matter in soil. When CAC is injected into the subsurface, the colloidal particles will be transported through porous media and will attach to sand grains adjacent to the injection point based on typical colloidal transport behavior. After injection, contaminant mass will be redistributed into a new three-phase system: aqueous phase, sorbed to organic matter, and sorbed to the CAC. Given the high sorption capacity of activated carbon, PFAS mass will likely be redistributed predominantly in the CAC-sorbed phase.

Typical sources contributing to PFAS plumes in the subsurface include back-diffusion from lower-permeability soils such as silt and clay; rate-limited desorption from organic matter in soil; percolation to the water table from a vadose zone source; and/or dissolution from nonaqueous phase liquid (NAPL) in which the PFAS has become entrained. If CAC is injected into a PFAS source zone, it is expected (at least conservatively) that these sources will continue to persist, resulting in long-term mass loading to the CAC zone over time. Because PFAAs are not expected to undergo transformation reactions, the adsorption capacity in a CAC zone will eventually become exhausted, resulting in the eventual breakthrough of PFAAs if the long-term source continues to persist.

A numerical model may help in estimating whether and/or when a regulatory cleanup level may be exceeded in the source zone or in a downgradient plume, depending on the specifics of the CAC injection. If or when PFAS breakthrough occurs, then remedial alternatives at that future time may include reinjection of CAC into or downgradient of the original CAC zone, or utilization of another *in situ* treatment technology that may become available in the future. The main benefit of *in situ* CAC as a mass flux reduction alternative, relative to pump-and-treat (P&T), which is the most common remedial technology implemented at PFAS sites, is the passive nature of an *in situ* CAC remedy and the corresponding lower cost at some sites.

Two numerical modeling approaches were developed and applied as part of this study to simulate the longevity of CAC (i.e., time until the regulatory cleanup goal is exceeded due to PFAS breakthrough), based on the single injection event at the site:

- Incorporation of a mass redistribution step into a three-dimensional (3-D) numerical reactive transport model referred to as the *In Situ*

Remediation Model, or ISR-MT3DMS, which is described by Carey, Chapman, Parker, and McGregor (2015) and

- Development of a simplified finite-difference solution in time to evaluate the time to reach breakthrough in the center of a PFAS source zone where advective and dispersive flux is low relative to the flux of sorption onto CAC.

4.1 | Simulating mass redistribution after CAC injection

Contaminant mass in the aqueous phase prior to CAC injection is calculated using

$$M_{w,o} = C_o\ \theta\ V_s \tag{3}$$

where $M_{w,o}$ is the mass in aqueous phase prior to CAC injection (mg); C_o is the aqueous concentration prior to CAC injection (mg/L); and V_s is representative soil volume (L).

Contaminant mass sorbed to organic matter in soil is determined using

$$M_{s,o} = K_{oc}\ f_{oc}\ C_o\ \rho_b\ V_s \tag{4}$$

where $M_{s,o}$ is the mass sorbed to organic matter in soil prior to CAC injection (mg) and f_{oc} is the fraction of organic carbon (g/g).

The total contaminant mass in soil (assuming there is no NAPL present) is given by

$$M_{T,o} = C_o\ V_s(\ \theta + K_{oc}\ f_{oc}\ \rho_b\ ) \tag{5}$$

where $M_{T,o}$ is the total mass in a representative soil volume prior to CAC injection (mg).

After injection of CAC into the subsurface, the contaminant mass will be redistributed within the CAC zone. It is assumed that aqueous PFAS will adsorb rapidly to the CAC, and that equilibrium desorption of PFAS from organic matter and subsequent sorption to CAC will occur. The actual time for desorption from organic matter to occur is uncertain and will vary based on site and contaminant conditions. However, as desorption does occur into the aqueous phase, the subsequent adsorption onto CAC is expected to be rapid due to the large surface area associated with CAC. This is consistent with a previous study that observed significantly faster equilibration times for a smaller activated carbon size (i.e., PAC versus GAC), due to a larger external surface area and more functional groups being available for PFAS sorption with the smaller carbon particle size (Yu et al., 2009).

A mass-balance approach was utilized to estimate the adjusted aqueous concentration (C_{adj}) in the CAC zone after injection. To facilitate this mass balance, it was assumed that at equilibrium after redistribution, the mass sorbed to organic matter and the mass in the aqueous phase are much smaller than the mass sorbed to CAC, immediately after CAC injection. Based on the large adsorption capacity as can be seen from the PFOS isotherms (Exhibit 5), this assumption is valid for the case study discussed here, as will be demonstrated below. This assumption should be verified on a site-by-site basis.

A mass-balance approach was utilized to estimate the adjusted aqueous concentration (C_{adj}) in the CAC zone after injection.

The mass sorbed to CAC after this redistribution step (i.e., immediately after CAC injection) is calculated using

$$M_{s,CAC} = K_f\ f_{cac} C_{adj}{}^{a}\ \rho_b\ V_s \tag{6}$$

where C_{adj} is the adjusted aqueous concentration after CAC injection (mg/L).

Based on the simplifying assumption described above, and by rearranging Equations (5) and (6), the adjusted aqueous concentration after CAC injection is calculated using

$$C_{adj} = \left[\frac{C_o\ (\ \theta + \ K_{oc}\ f_{oc}\ \rho_b\ )}{K_f\ \ f_{cac}\ \rho_b}\right]^{1/a} \tag{7}$$

Using the maximum observed PFOS concentration (1.5 μg/L) at the Central Canada site as an example for C_o, the adjusted aqueous concentration after CAC injection may be calculated using Equation (6). The PFOS-CAC isotherm determined based on the PFAS mixture from a former fire-training area is used as the base case for this calculation and for the longevity modeling presented below. Based on an effective porosity (θ) of 20%, K_{oc} = 920 mg$^{1\text{-}a}$ L^a/kg (refer to Supporting Information), f_{oc} = 0.1% based on the minimum f_{oc} that represents dissolved organic carbon sorption (Delle Site, 2001), ρ_b = 1.6 g/mL, K_f = 4,900 mg$^{1\text{-}a}$ L^a/kg, a = 0.24, and f_{cac} = 0.02%, C_{adj} is calculated to be 2×10^{-9} μg/L, which corresponds to the PFOS concentration that would occur after mass is redistributed due to CAC injection.

The retardation coefficient corresponding to linear sorption to organic matter is calculated using the above parameters to be 8.4. This is orders of magnitude lower than the retardation coefficient calculated using Equation (2) for sorption of PFOS to CAC ($R_{cac} = 1 \times 10^9$), which illustrates that mass in the aqueous and organic matter-sorbed phases is negligible relative to the CAC-sorbed phase immediately after injection. The difference in retardation coefficients for organic matter and CAC adsorption supports that the simplifying assumption in the mass balance approach is reasonable for this site.

4.2 | Equilibrium mixing model

A transient EMM was developed to provide an approximate estimate of how long the CAC remedy would remain effective in the middle of a PFAS source zone (i.e., prior to breakthrough above regulated concentration limits). The EMM is based on a mass balance implemented using a finite-difference solution in time. The EMM is also based on the assumption that there is ongoing PFAS mass discharge into groundwater in the source zone after CAC injection, due to contributions from

back-diffusion, rate-limited desorption, infiltration to the water table from a source in the vadose zone, and/or NAPL dissolution. The mass discharge term in the EMM may also represent the plume strength directly upgradient of a reactive barrier where CAC is injected to intercept a plume.

The EMM simulates the aqueous concentration over time in a single mixing cell in the middle of a source zone. The net fluxes into and out of the grid cell due to advection and dispersion are assumed to be equal, resulting in accumulation in the cell due to mass discharge from the source. The EMM is applicable when the rate of sorptive flux onto the CAC is significantly larger than the net advective and dispersive out of the mixing cell. The EMM simulates the aqueous concentration over time in the mixing cell, accounting for sorption to CAC. Results of this model may be used to estimate the earliest time at which breakthrough may occur due to long-term loading of PFAS mass within the CAC zone. The benefit of this finite-difference solution is that it can be implemented within a spreadsheet, so a more sophisticated numerical model is not required to develop a preliminary estimate of CAC longevity in the source zone. The limitation of this approach is that it will underestimate the longevity in areas where the net advective and dispersive fluxes out of the grid cell are relatively significant.

The EMM is applicable when the rate of sorptive flux onto the CAC is significantly larger than the net advective and dispersive out of the mixing cell.

The initial aqueous concentration in the model at a time of 0 (C_{adj}) is calculated based on Equation (7). At time step t, the change in aqueous concentration, and the retardation coefficient in the grid cell, are calculated using

$$R^t = 1 + \frac{\rho_b}{\theta} K_f f_{cac} a (C^{t-1})^{a-1} \quad (8)$$

$$\Delta C^t = \left(Md^t_{src} \Delta t\right) / \left(V_{cell} R^t \theta\right) \quad (9)$$

$$C^t = C^{t-1} + \Delta C^t \quad (10)$$

where R^t is the retardation coefficient at the current time step; C^{t-1} is the aqueous concentration at the previous time step (mg/L); ΔC^t is change in aqueous concentration at the current time step (mg/L); C^t is aqueous concentration at the current time step (mg/L); $Md_{src}{}^t$ is source mass discharge into the grid cell at the current time step (mg/d); Δt is time step duration (d); and V_{cell} is the volume of the cell (L).

The EMM includes functionality for representing an exponential decline over time in the source zone mass discharge (Md_{src}), to represent sources that deplete over time. For example, examination of results from an analytical solution for back-diffusion indicated that a back-diffusion source decline half-life of 20 to 30 years is reasonable for some sites (refer to Supporting Information).

Because the EMM does not represent flux leaving the cell by advection or dispersion, the simulated aqueous concentrations will eventually exceed the initial aqueous concentration. A check is included in the EMM to detect when the simulated aqueous concentration reaches the maximum observed concentration prior to CAC injection. It is also possible to represent an exponential decline in this maximum initial concentration in the EMM based on the source decline discussed above, using the same half-life as the source zone mass discharge (Md_{src}).

As shown below, for the cases examined here, the results from the EMM model are similar to the results from ISR-MT3DMS, which accounts for PFAS transport by advection and dispersion in the source zone.

5 | *IN SITU* CAC LONGEVITY ASSESSMENT

The models described above (ISR-MT3DMS and the EMM) were used to predict the longevity of *in situ* CAC effectiveness at the Central Canada site in the middle of the source area and at the downgradient extent of the CAC zone, which is approximately 10 m downgradient of the source area. Longevity is defined in this study to represent the time between CAC injection and when the PFOS concentration exceeds the regulatory cleanup level. For this study, the regulatory cleanup level was assumed to be the Health Canada drinking water screening value for PFOS of 0.6 μg/L.

5.1 | Flow and transport model construction

A 2-D areal model domain was constructed to represent groundwater flow and solute transport at the site. MODFLOW (McDonald & Harbaugh, 1988) was used to simulate steady-state groundwater flow based on the average site characteristics for hydraulic conductivity (2.6 m/d). The model grid was based on a consistent 2 m spacing outside of the CAC zone, and 0.5 m within the CAC zone with a transition spacing of 1 m between these two areas. A uniform saturated thickness of 0.8 m was assumed, consistent with the thickness of the PFAS plume at the site (McGregor, 2018). Constant head boundary conditions were used to replicate the observed average horizontal hydraulic gradient of 0.06 m/m. Because the area was industrial and mostly covered at the ground surface, it was assumed that the rate of infiltration was zero except for a small rate used in the source area of 0.1 inch/year, which was used to simulate a PFAS mass discharge in the source area when coupled with the reactive transport model.

The ISR-MT3DMS reactive transport model was first used to simulate the development of a relatively steady PFOS plume just prior to CAC injection, modeled to occur at a simulation time of 1,500 days. The transport model utilized a time step of 1 day. The longitudinal and transverse horizontal dispersivities were simulated to be 1 m and

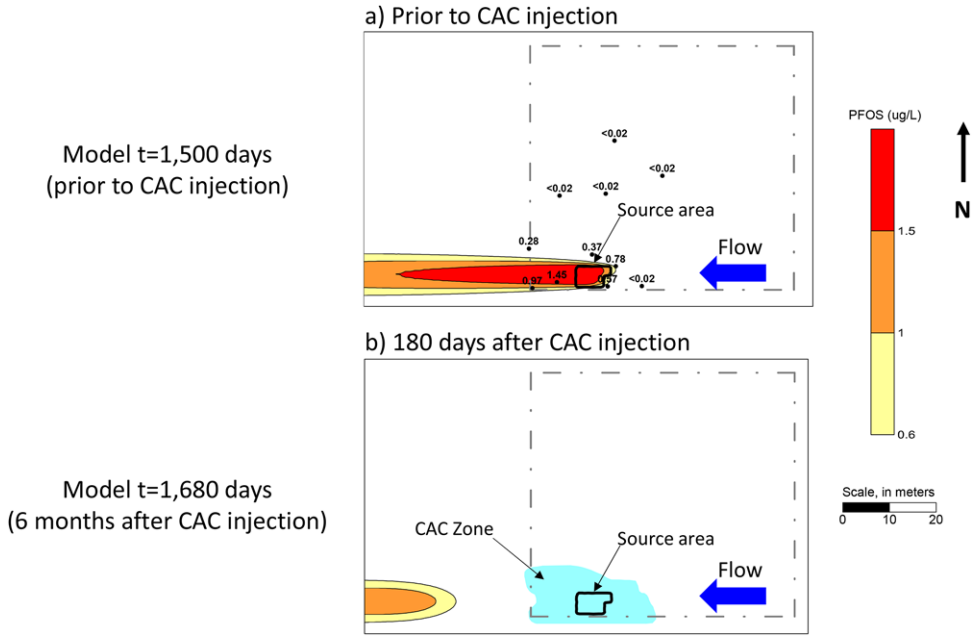

EXHIBIT 7 Simulated plume detachment after CAC injection for baseline case. The minimum PFOS concentration contour of 0.6 μg/L is based on the drinking water screening value adopted by Health Canada (July 2018). PFOS in the CAC zone is simulated to be below analytical detection limits

0.1 m, respectively. The source area mass discharge was calibrated to provide a general match to the PFOS plume observed at the site. Exhibit 7a shows the simulated PFOS plume based on a calibrated source area mass discharge rate of approximately 0.6 gram per year over a source area of 30 m^2. Observed preinjection PFOS monitoring well concentrations are also shown in Exhibit 7a, demonstrating that there is a reasonable match between the simulated and observed plumes prior to CAC injection.

A mass discharge decline half-life of 30 years was specified to represent a gradual decline in mass discharge over time. (ISR-MT3DMS provides the option to simulate an exponential decline rate for recharge sources.) The ISR-MT3DMS model incorporating Equation (7) was used to calculate the postinjection aqueous PFOS concentration, immediately after the redistribution of mass. In the ISR-MT3DMS model, the linear sorption isotherm was used to represent sorption to organic matter outside the CAC zone at all times, and within the CAC zone prior to the simulated injection time of 1,500 days. The Freundlich isotherm was used to simulate PFOS sorption to CAC in the mass flux reduction zone after the simulation time of 1,500 days.

The extent of the CAC zone was defined as an input to the model based on the locations of the temporary injection wells. As discussed above, the radius of influence for CAC was conservatively assumed to be 3 m around each injection point, which is less than the distribution of CAC during postinjection monitoring. The PFOS-CAC isotherm for the PFAS mixture from the former fire-training area was utilized for the base-case simulations (K_f = 4,900 mg^{1-a} L^a/kg and a = 0.24). There is uncertainty in the site-specific PFOS-CAC isotherm that is representative of the Central Canada site, relative to the isotherm determined for the former fire-training area. These model simulations are conducted to illustrate the sensitivity of CAC longevity to various parameters, and to evaluate if the range in possible Freundlich isotherm properties may be narrowed by comparing model simulations to observed conditions post-CAC injection.

For the base-case model simulation, an f_{cac} of 0.02% was used, based on the average f_{cac} measured at the site (McGregor, 2018). Other transport model parameters are consistent with those described above for the example PFOS C_{adj} calculation. The total simulation period extended to 100 years after CAC injection, for a total simulation time of 38,000 days.

Exhibit 7b presents the simulated PFOS plume at a time of 180 days after CAC injection (i.e., total simulation time of about 1,680 days). The minimum concentration contour (0.6 μg/L) represents the Health Canada PFOS screening value. Simulated concentrations in the CAC zone were orders of magnitude below the PFOS detection limit, due to the high CAC adsorption capacity for PFOS. The model simulation is consistent with groundwater sampling conducted at monitoring wells within the CAC 6 months after CAC injection, where PFOS was not detected at any wells with a detection limit of 0.03 μg/L. Exhibit 7b also demonstrates the simulated detachment of the PFOS plume downgradient of the CAC zone, which was caused by the effective sorption of PFOS within the CAC zone.

Exhibit 8a shows the preinjection PFOS mass distribution on the site, which illustrates that most of the PFOS mass was sorbed to organic matter, and only a small proportion of PFOS mass was in the aqueous phase. This is consistent with the preinjection retardation coefficient of 8.4 for PFOS. Exhibit 8b shows the total PFOS mass distribution within the CAC zone, after equilibration with CAC according to Equation (7). Exhibit 8b demonstrates that PFOS mass is almost entirely sorbed to CAC. Within the CAC zone and prior to CAC injection, the model simulated a total PFOS mass of 30.4 mg in the aqueous phase and 223.5 mg sorbed to native organic matter, for a total mass of 253.9 mg. Immediately after CAC injection, ISR-MT3DMS simulated

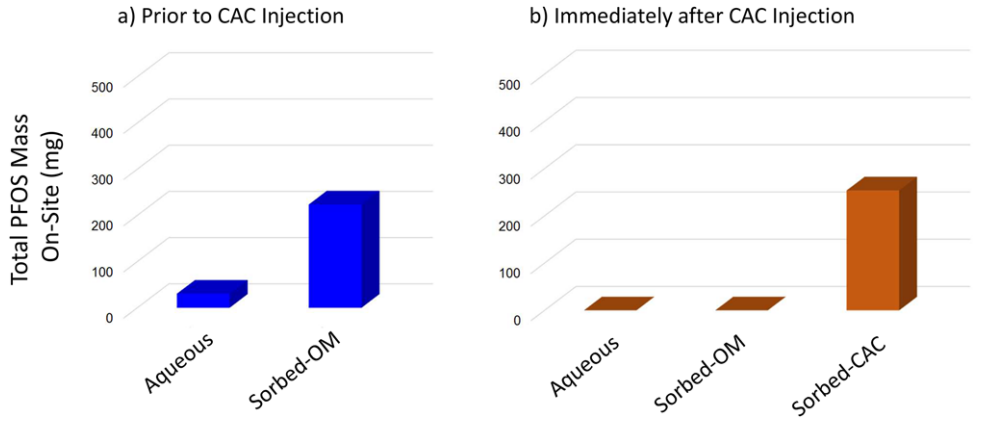

EXHIBIT 8 PFOS mass-balance pre- and post-CAC injection. Sorbed-OM refers to PFOS sorbed to native organic matter

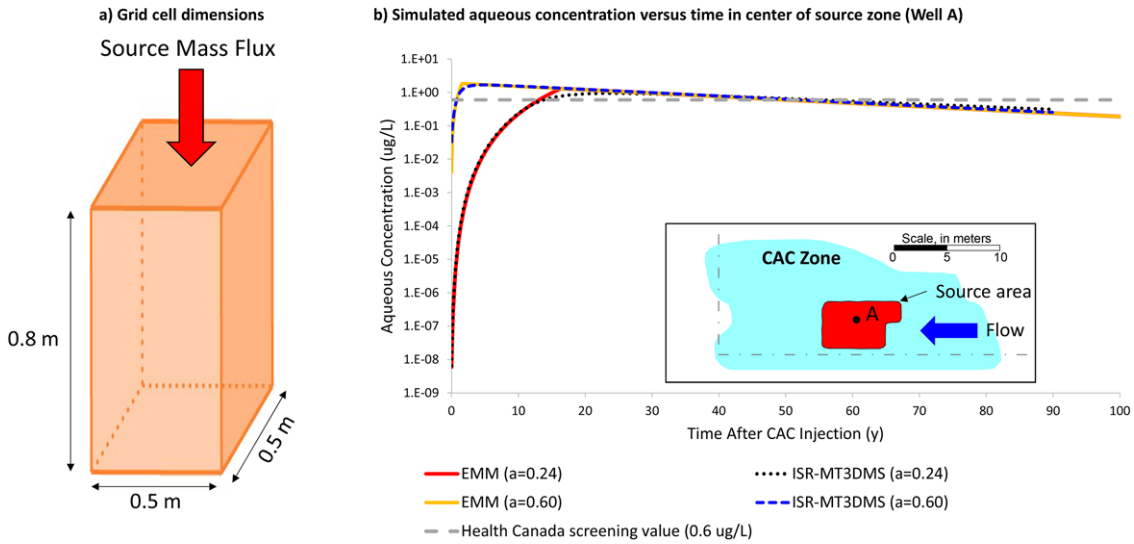

EXHIBIT 9 Comparison of EMM and ISR-MT3DMS simulated concentrations versus time in the center of the source area. ISR-MT3DMS simulated concentrations are at observation well A shown on the inset map. f_{cac} for simulations was 0.02%

the total PFOS mass in this same area to be 1.0×10^{-7} mg in the aqueous phase, and 7.4×10^{-7} mg sorbed to native organic matter. PFOS mass sorbed to CAC was simulated to be approximately 253.9 mg. This distribution confirms the mass balance assumption that the mass in the aqueous and native organic matter-sorbed phases is negligible relative to the mass sorbed to CAC.

5.2 | CAC longevity modeling

5.2.1 | Breakthrough time at center of source area (EMM versus ISR-MT3DMS)

The EMM solution (i.e., Equations (8)–(10)) results were compared with ISR-MT3DMS simulations that include advective and dispersive fluxes across the source area.

Exhibit 9a shows the dimensions of the single grid cell modeled using the EMM, where only the source discharge is considered as a cumulative flux into the grid cell. The length and width of the EMM grid cell are consistent with the grid resolution in ISR-MT3DMS (i.e., 0.5 m × 0.5 m, and the saturated thickness of the grid cell is 0.8 m). Two different scenarios were used for comparison of the EMM and ISR-MT3DMS under a range of longevity conditions in the source area: one with Freundlich exponent $a = 0.24$ (base case) and one with $a = 0.6$ (representing the exponent determined for a pure PFOS solution isotherm). Both scenarios used $K_f = 4{,}900$ mg^{1-a} L^a/kg, $f_{cac} = 0.02\%$, and a source mass discharge decline half-life of 30 years.

Exhibit 9b compares the EMM and ISR-MT3DMS simulated concentrations in the center of the source zone for these two scenarios. The location of the observation well specified in ISR-MT3DMS (well A) is shown in the inset map in Exhibit 9b. Exhibit 9b demonstrates that the simulated PFOS concentrations over time in the EMM were similar to the results from ISR-MT3DMS, which indicates that the EMM assumption of negligible advective and dispersive fluxes relative to the CAC sorption flux is reasonable for the center of the source area at this site.

The base-case scenario ($a = 0.24$) resulted in a breakthrough time of approximately 14 years, corresponding to the time after CAC injection when the simulated PFOS concentration exceeded the Health Canada screening value of 0.6 μg/L. However, as shown below, the breakthrough time at the downgradient extent of the CAC zone (10 m downgradient of the source area) is much longer than the breakthrough time

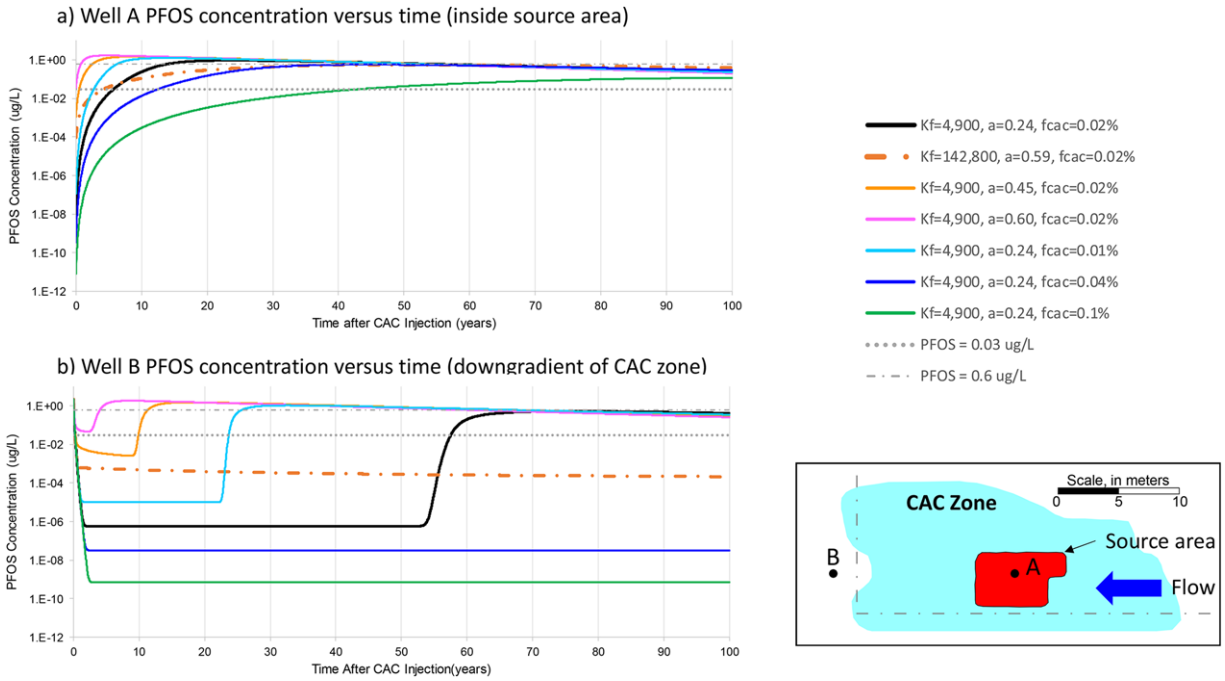

EXHIBIT 10 Breakthrough timeframe sensitivity analysis. $t = 0$ corresponds to when CAC injection was simulated. K_f units are mg^{1-a} L^a/kg

in the source area. Therefore, the EMM has limited applicability when a CAC buffer zone is incorporated downgradient of the source area and may significantly underestimate the longevity in this case. As a comparison, the breakthrough time corresponding to a greater Freundlich exponent of $a = 0.6$ is only 0.8 year, indicating that this exponent has a significant influence on the sorption of PFOS and the longevity of a CAC remedy.

5.2.2 | Breakthrough time at downgradient boundary of the CAC zone (ISR-MT3DMS)

Exhibits 10a and 10b present simulated PFOS concentrations versus time at two observation wells in the model domain: well A in the source zone and well B directly downgradient of the CAC zone. The base-case simulation utilized the PFOS isotherm determined with the PFAS groundwater mixture ($K_f = 4{,}900$ mg^{1-a} L^a/kg and $a = 0.24$) and $f_{cac} = 0.02\%$. Three additional isotherm scenarios were simulated to evaluate the sensitivity of the breakthrough curves to isotherm parameters (all using $f_{cac} = 0.02\%$): (1) $K_f = 142{,}800$ mg^{1-a} L^a/kg and $a = 0.59$ (PFOS pure solution isotherm); (2) $K_f = 4{,}900$ mg^{1-a} L^a/kg and $a = 0.45$; and (3) $K_f = 4{,}900$ mg^{1-a} L^a/kg and $a = 0.60$. Three additional scenarios were simulated using the base-case isotherm and f_{cac} values of 0.01%, 0.04%, and 0.1%.

Exhibit 10a shows that PFOS concentrations in the source zone increase above the detection limit of 0.03 μg/L at a time of 5.7 years after CAC injection, and increases above the Health Canada screening value of 0.6 μg/L after 14 years. In comparison, the scenario using $K_f = 4{,}900$ mg^{1-a} L^a/kg and $a = 0.45$ resulted in a detectable PFOS concentration in the source zone at a time of 0.5 years after CAC injection, and the scenario using $a = 0.60$ always had detectable PFOS in the source zone. These two isotherm scenarios do not match site conditions where PFOS was not detected in any site monitoring wells over the two-year period since CAC injection, with the exception of one low detection that may have been due to cross-contamination. Therefore, these two isotherms are not representative of the sorption characteristics of CAC in the geochemical conditions at this site.

Exhibit 10b illustrates the PFOS concentration versus time curves for well B, which is 3.2 m downgradient of the CAC zone and 11.7 m downgradient of the source area. Comparison of the curves in Exhibits 10a and 10b shows that breakthrough occurs much later at well B than at well A (in the source area). For example, PFOS exceeds the detection limit at well A in the source area at a time of 5.7 years after CAC injection, but only exceeds the detection limit at well B after 62 years. This delay in the downgradient breakthrough is due to the 10 m long CAC buffer zone downgradient of the source area. This demonstrates the benefit that may be derived by extending the length of the CAC buffer zone (parallel to groundwater flow) on the longevity of an *in situ* CAC remedy, or by increasing the retention time in a permeable CAC barrier wall being used to intercept a PFAS plume. The model can be used to investigate various schemes for CAC-based remediation and for conducting cost–benefit analyses.

The base-case scenario in Exhibit 10b shows that the PFOS concentration does not exceed the Health Canada screening value of 0.6 μg/L, even though concentrations did eventually rise at well B, because the source mass discharge was simulated to have a decline half-life of 30 years. This base-case simulation predicts that the *in situ* CAC remedy will be successful at mitigating future plume migration downgradient of the site. There is uncertainty regarding this outcome, related to uncertainty in the *in situ* PFOS-CAC isotherm, mass discharge decline half-life, and even in future regulatory cleanup levels, which may be significantly lower than 0.6 μg/L. However, given the relatively low cost to implement the CAC remedy at this site, and the ability to adapt the

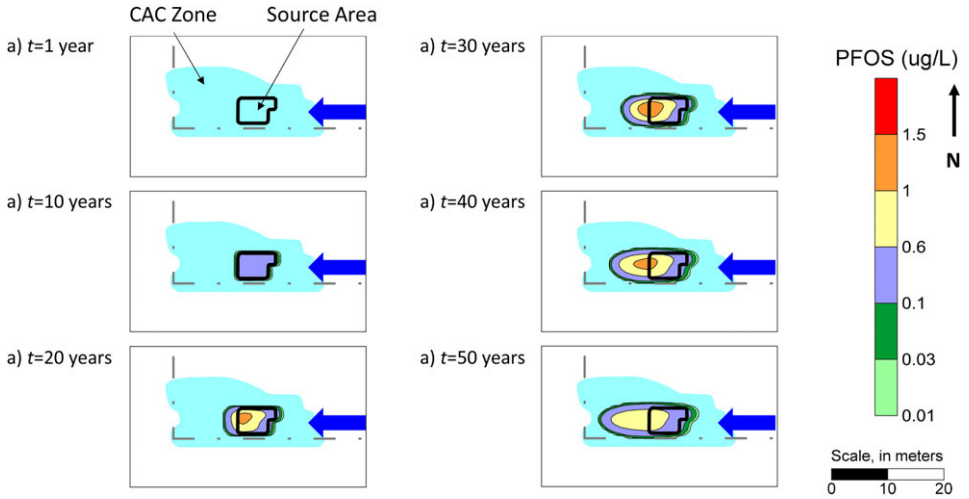

EXHIBIT 11 PFOS concentration contours over time. $K_f = 4{,}900\ mg^{1-a}\ L^a/kg$, $a = 0.24$, and $f_{cac} = 0.02\%$. Light blue shading represents the CAC zone and the thick black outline represents the source area. The dashed line represents the site boundary. Times correspond to the time after CAC injection. See Exhibit 1 for site monitoring well locations

remedy in the future by reinjecting into the existing CAC zone or to extend the length of the CAC buffer zone, this remedy may be viable at other PFAS sites. The only other alternative presently available at PFAS sites is P&T that would have to be operated for decades due to the ongoing nature of the PFAS source. It is also possible to combine P&T in a remedy, such as using P&T at a site boundary where PFAS concentrations are higher, and implementing CAC barriers downgradient to mitigate plume migration.

Exhibit 10b also demonstrates the influence that f_{cac} has on the remedy longevity. PFOS exceeds the detection limit at well B at a time of 24 years after CAC injection when the average f_{cac} is 0.01%, which is approximately 60% sooner than the scenario using $f_{cac} = 0.02\%$. Breakthrough did not occur at well B during the 100-year simulation for $f_{cac} = 0.04\%$ and 0.1%. This demonstrates that the longevity of the *in situ* CAC remedy may be engineered by increasing f_{cac} and the corresponding CAC concentration in the injected solution. Alternatively, the length of the CAC zone can be extended in the future based on long-term monitoring results to transfer a portion of the remedy cost into the future.

Exhibit 11 presents simulated PFOS concentration contours for the base-case scenario at simulation times of 1, 10, 20, 30, 40, and 50 years after CAC injection. The minimum PFOS concentration contour is 0.03 μg/L, which represents the PFOS detection limit. At t = 1 year after CAC injection, simulated PFOS concentrations are below the detection limit throughout the CAC zone, which is consistent with observed conditions. At a time of 10 years, PFOS is predicted to be detectable within the source area but still below the Health Canada screening value of 0.6 μg/L. At this time, PFOS is predicted to remain below the detection limit outside of the source area.

As concentrations continue to increase in the source area with time, the concentrations downgradient of the source area begin to increase above 0.6 μg/L. Expansion of the plume beyond the source area is slow due to retardation from sorption to CAC in the downgradient buffer zone. Two observation points were used in the model to estimate the rate of retardation of the front of the plume, which is defined for this assessment as the contour representing the PFOS detection limit of 0.03 μg/L. Both observation points are on a flow path within the CAC zone; one observation point is situated 2 m downgradient of the source area, and the second observation point is situated 5 m downgradient of the first point. The front of the plume reached the first point on the flow path at a time of 18.4 years after CAC injection, and the plume front reached the second point at a time of 40.4 years. This corresponds to an average retardation coefficient of 1,250 for the plume front within the CAC zone, downgradient of the source area.

Installing monitoring wells in the CAC buffer zone would allow detection of PFAS migration. Given the slow transport through the CAC buffer zone, there would be sufficient time to implement additional measures to slow plume movement, such as injection of additional CAC or other alternatives.

6 | CONCLUSIONS AND RECOMMENDATIONS

Various visualization and modeling methods were used to evaluate the performance of *in situ* CAC at a PFAS site in Central Canada. Redox radial diagrams demonstrate that redox conditions within and downgradient of the source area were aerobic as a result of the oxygen-releasing materials included with the injected solution. Monitoring data indicate that this did not influence the effectiveness of the CAC remedy with respect to PFAS immobilization.

Laboratory isotherms were derived for two solutions mixed with CAC: (1) PFOS in 1 mM $NaHCO_3$ and (2) a groundwater sample with PFOS among other PFAS from a former fire-training area in the United States. The isotherm parameters for the pure PFOS solution were $K_f = 142{,}800\ mg^{1-a}\ L^a/kg$ and $a = 0.59$, and the isotherm for the PFAS groundwater sample had $K_f = 4{,}900\ mg^{1-a}\ L^a/kg$ and $a = 0.24$. The difference between these two isotherms is likely related to the effects of competitive sorption due to the presence of other PFAS, native organic matter, and/or other co-contaminants in the groundwater

sample. Isotherm differences may also be related to geochemical differences between the two solutions used. The effects of competitive sorption and geochemistry on CAC isotherms require further study. It is recommended that site-specific PFAS-CAC isotherms be determined to reduce uncertainty in longevity predictions.

A mass-balance approach was developed to facilitate the numerical modeling of mass redistribution after CAC injection, when mass transitions from a two-phase system (aqueous and sorbed to organic matter) to a three-phase system, which also includes mass sorbed to CAC. A simplifying assumption in this mass balance is verified to be applicable at this site, whereby the redistributed mass after CAC injection is predominantly in the CAC-sorbed phase.

An EMM was developed to simulate aqueous concentrations over time in a single grid cell in the center of a PFAS source area after CAC injection, based on a mass balance. The EMM is demonstrated, based on comparison with ISR-MT3DMS, to be applicable in areas where advective and dispersive fluxes are low relative to the CAC sorptive flux.

The redistribution mass-balance approach was incorporated into a 3-D reactive transport model (ISR-MT3DMS), to facilitate an assessment of the longevity of *in situ* CAC within and downgradient of a source area. ISR-MT3DMS simulations indicate that the remedy will be effective in the long-term at the site with respect to PFOS, in part because of the relatively high Health Canada screening value for PFOS of 0.6 μg/L.

As with any long-term model prediction, there is uncertainty with these results, primarily with respect to the *in situ* isotherm parameters (K_f and a). A sensitivity analysis was used to demonstrate that several possible isotherms were not realistic because the model simulations were inconsistent with observed conditions. Model results also showed that the plume front is highly retarded within the CAC zone. Implementation of a CAC buffer zone downgradient of a contaminant source area provides an important opportunity for conducting long-term monitoring to confirm when additional CAC injection is required. The model was also used to demonstrate that *in situ* CAC longevity may be engineered by adjusting the CAC concentration in the injected solution, assuming that f_{cac} is proportional to the injected solution concentration.

Given the relatively low cost to implement the CAC remedy at this site, and the ability to adapt the remedy in the future by reinjecting into the existing CAC zone or to extend the length of the CAC buffer zone, this remedy may be viable at other PFAS sites. The only other alternative presently available at PFAS sites is P&T that would have to be operated for decades due to the ongoing nature of the PFAS source. It is also possible to combine P&T and CAC in a site management strategy, such as using P&T at a site boundary where PFAS concentrations are higher, and implementing CAC barriers downgradient to mitigate plume migration.

ACKNOWLEDGMENTS

The authors would like to thank Dr. Kristen Thoreson and Dr. Jeremy Birnstingl at Regenesis for their insightful comments during this study. We would also like to thank Dr. Charles Schaefer at CDM Smith for providing the PFAS groundwater sample.

REFERENCES

Appleman, T. D., Higgins, C. P., Quinones, O., Vanderford, B. J., Kolstad, C., Zeigler-Holady, J. C., & Dickenson, E. R. V. (2014). Treatment of poly- and perfluoroalkyl substances in U.S. full-scale water treatment systems. *Water Research*, *51*, 246–255.

Avendano, S. M., & Liu, J. (2016). Production of PFOS from aerobic soil biotransformation of two perfluoroalkyl sulfonamide derivatives. *Chemosphere*, *119*, 1084–1090.

Carey, G. R., Chapman, S. W., Parker, B. L., & McGregor, R. (2015). Application of an adapted version of MT3DMS for modeling back-diffusion remediation timeframes. *Remediation Journal*, *25*(4), 55–79.

Carey, G. R., Van Geel, P.J., Wiedemeier, T. H., & McBean, E. A. (2003). A modified radial diagram approach for evaluating natural attenuation trends for chlorinated solvents and inorganic redox indicators. *Ground Water Monitoring & Remediation*, *23*(4), 75–84.

Carey, G. R., Wiedemeier, T. H., Van Geel, P. J., McBean, E. A., Murphy, J. R., & Rovers, F. A. (1999). SEQUENCE visualization of natural attenuation trends at Hill Air Force Base, Utah. *Bioremediation Journal*, *3*(4), 379–393.

Delle Site, A. (2001). Factors affecting sorption of organic compounds in natural sorbent/water systems and sorption coefficients for selected pollutants: A review. *Journal of Physical and Chemical Data Review*, *30*(1), 187–439.

Harding-Marjanovic, K. C., Houtz, E. F., Yi, S., Field, J. A., Sedlak, D. L., & Alvarez-Cohen, L. (2015). Aerobic biotransformation of fluorotelomer thioether amido sulfonate (Lodyne) in AFFF-amended microcosms. *Environmental Science & Technology*, *49*(13), 7666–7674.

Hatton, J., Holton, C., & DiGuiseppi, B. (2018). Occurrence and behavior of per- and polyfluoroalkyl substances from aqueous film-forming foam in groundwater systems. *Remediation Journal*, *28*(2), 89–99.

Health Canada. (2018). Drinking water screening values: Perfluoroalkylated substances. *Water Talk*. Retrieved from https://www.canada.ca/en/services/health/publications/healthy-living/water-talk-drinking-water-screening-values-perfluoroalkylated-substances.html

McCleaf, P., Englund, S., Ostlund, A., Lindegren, K., Wiberg, K., & Ahrens, L. (2017). Removal efficiency of multiple poly- and perfluoroalkyl substances (PFASS) in drinking water using granular activated carbon (GAC) and anion exchange (AE) column tests. *Water Research*, *120*, 77–87.

McDonald, M. G., & Harbaugh, A. W. (1988). *A modular three-dimensional finite difference ground-water flow model* (586 pp.). Reston, VA: U.S. Geologic Survey. https://doi.org/10.3133/twri06A1

McGregor, R. (2018). In situ treatment of PFAS-impacted groundwater using colloidal activated carbon. *Remediation Journal*, *28*, 33–41.

Porewater Solutions. (2017). *Visual Bio™ radial ciagrams for visualizing natural and enhanced chemical degradation trends: V1.1 user's guide*. Ottawa, Ontario: Porewater Solutions.

Regenesis. (2016). *PlumeStop® technical bulletin 5.1: In situ containment of PFOA and PFOS using PlumeStop® Liquid Activated Carbon™*. San Clemente, CA: Author.

U.S. Environmental Protection Agency (USEPA). (2018, April). *Remedial technology fact sheet – Activated carbon-based technology for in situ remediation, EPA 542-F-18-001*. Washington, DC: Author.

U.S. Environmental Protection Agency (USEPA). (2016a). Drinking water health advisory for perfluorooctane sulfonate (PFOS). Retrieved from https://www.epa.gov/sites/production/files/2016-05/documents/pfos_health_advisory_final_508.pdf

U.S. Environmental Protection Agency (USEPA). (2016b). Drinking water health advisory for perfluorooctanoic acid (PFOA). Retrieved from https://www.epa.gov/sites/production/files/2016-05/documents/pfoa_health_advisory_final-plain.pdf

Yu, Q., Zhang, R., Deng, S., Huang, J., & Yu, G. (2009). Sorption of perfluorooctane sulfonate and perfluorooctanoate on activated carbons and resin: Kinetic and isotherm study. *Water Research*, *43*, 1150–1158.

AUTHORS' BIOGRAPHIES

Grant R. Carey, PhD, P Eng, is President of Porewater Solutions in Ottawa, Ontario. Dr. Carey specializes in groundwater modeling, NAPL characterization and remediation, contaminant transport, back-diffusion, and environmental forensics. Dr. Carey also founded the PFAS Remediation Research Group. He received a BASc from the University of Waterloo, an M Eng from Carleton University, and a PhD from the University of Guelph.

Rick McGregor, MSc, MBA, is a hydrogeologist with In Situ Remediation Services Ltd based in Canada. McGregor has a BSc in geology and MSc in hydrogeology and geochemistry from the University of Waterloo along with an MBA from Wilfrid Laurier University. Rick has over 27 years of experience in research, consulting, and contracting. His current focus is on the remediation of impacted groundwater.

Anh Le-Tuan Pham, PhD, is an Assistant Professor of Civil and Environmental Engineering at the University of Waterloo. His research group investigates contaminant fate and transformation. The current research focuses on developing novel technologies for the remediation of contaminated soil and groundwater, treatment of oil sands process water, and removal of emerging contaminants. He received his BS in Chemical Engineering from the Hanoi University of Technology, and MS and PhD in Civil and Environmental Engineering from the University of California, Berkeley.

Brent Sleep, PhD, P Eng, conducts hybrid research with laboratory experimentation, field studies, and computer modeling to determine the fate and transport of organic chemicals in the subsurface and surface aquatic environments. More specifically, Dr. Sleep's research is dedicated to developing innovative methods for remediation of soil and groundwater contamination, with a focus on organic contaminants. His research group is working on a variety of *in situ* subsurface remediation methods, conducting laboratory and computer modeling studies of bioremediation, thermal remediation, and the applications of chemical oxidants and nanoscale zero valent iron for subsurface remediation. His group is also investigating the transport of pathogens in fractured rock aquifers. Dr. Sleep received a BASc, MASc, and PhD from the University of Waterloo.

Seyfollah Gilak Hakimabadi, MS, is a PhD student in the Department of Civil and Environmental Engineering at the University of Waterloo. He received a BS in Chemical Engineering from the Amirkabir University of Technology, and an MS in Chemical Engineering from the Ferdowsi University of Mashhad.

SUPPORTING INFORMATION

Additional supporting information may be found online in the Supporting Information section at the end of the article.

How to cite this article: Carey GR, McGregor R, Pham AL-T, Sleep B, Hakimabadi SG. Evaluating the longevity of a PFAS *in situ* colloidal activated carbon remedy. *Remediation*. 2019;29:17–31. https://doi.org/10.1002/rem.21593

DOI: 10.1002/rem.21741

RESEARCH ARTICLE

WILEY

Longevity of colloidal activated carbon for in situ PFAS remediation at AFFF-contaminated airport sites

Grant R. Carey[1] | Seyfollah G. Hakimabadi[2] | Mantake Singh[3] | Rick McGregor[4] | Claire Woodfield[3] | Paul J. Van Geel[3] | Anh Le-Tuan Pham[2]

[1]Porewater Solutions, Ottawa, Ontario, Canada

[2]Department of Civil and Environmental Engineering, University of Waterloo, Ontario, Waterloo, Canada

[3]Department of Civil and Environmental Engineering, Carleton University, Ontario, Ottawa, Canada

[4]In Situ Remediation Services Ltd., St. George, Ontario, Canada

Correspondence
Grant R. Carey, Porewater Solutions, 2958 Barlow Crescent, Ottawa, ON K0A 1T0, Canada.
Email: gcarey@porewater.com

Funding information
Porewater Solutions, Ontario Centers for Excellence, and Natural Sciences and Engineering Research Council

Abstract

A review of state per- and polyfluoroalkyl substances (PFAS) guidelines indicates that four long-chain PFAS (perfluorooctanesulfonic acid [PFOS] and perfluorooctanoic acid [PFOA] followed by perfluorohexanesulfonic acid [PFHxS] and perfluorononanoic acid [PFNA]) are the most frequently regulated PFAS compounds. Analysis of 17 field-scale studies of colloidal activated carbon (CAC) injection at PFAS sites indicates that in situ CAC injection has been generally successful for both short- and long-chain PFAS in the short-term (0.3–6 years), even in the presence of low levels of organic co-contaminants. Freundlich isotherms were determined under competitive sorption conditions using a groundwater sample from an aqueous film-forming foam (AFFF)-impacted site. The median concentrations for these PFAS of interest at 96 AFFF-impacted sites were used to estimate influent concentrations for a CAC longevity model sensitivity analysis. CAC longevity estimates were shown to be insensitive to a wide range of potential cleanup criteria based on modeled conditions. PFOS had the greatest longevity even though PFOS is present at higher concentrations than the other species because the CAC sorption affinity for PFOS is considerably higher than PFOA and PFHxS. Longevity estimates were directly proportional to the CAC fraction in soil and the Freundlich K_f, and were inversely proportional to the influent concentration and average groundwater velocity.

1 | INTRODUCTION

Per- and polyfluoroalkyl substances (PFAS) have been widely used on a global level for many decades. Perhaps the greatest source of PFAS contamination in the environment today is the use of aqueous film-forming foams (AFFF) for putting out fires. A large number of military and civilian airports have PFAS soil and groundwater contamination due to historical fire training activities. PFAS include polyfluoroalkyl precursors and recalcitrant perfluoroalkyl acids (PFAAs). PFAAs consist of two classes: perfluorosulfonates (PFSAs) and perfluorocarboxylates (PFCAs). The fluorocarbon chain length of these PFAAs affects the relative toxicity and hydrophobicity of these compounds. The widespread occurrence of PFAS in the subsurface, combined with their recalcitrance and toxicity, presents a significant groundwater remediation challenge. This challenge is compounded by uncertainty in future regulatory changes anticipated at the federal and state levels, regarding which individual PFAS will be regulated and corresponding clean-up goals.

The most common approach used today for the remediation of PFAS in groundwater involves groundwater extraction with ex situ

treatment, using granular activated carbon (GAC) or ion exchange resins to facilitate adsorption-based PFAS treatment. Another technology that has recently been gaining acceptance is the injection of colloidal activated carbon (CAC) into an aquifer to enhance the in situ adsorption of PFAS. CAC may be adopted as an interim or final remedy at some sites, to prevent the ongoing PFAS mass flux into a downgradient plume (e.g., see McGregor, 2018).

Implementation of CAC as an in situ remediation approach for PFAS in groundwater involves the injection of an organic polymer-stabilized solution containing CAC through temporary injection wells. REGENESIS distributes a patented CAC-containing solution called PlumeStop™. This solution includes an organic polymer that helps to facilitate the transport of CAC some distance away from the injection location. CAC will physically attach to grains of soil based on traditional colloidal transport behavior.

Aqueous PFAS contamination is transported with groundwater into the CAC sorption zone, where it will adsorb to CAC attached to soil particles. After CAC injection, the ongoing mass loading of PFAS and other co-occurring compounds into the CAC sorption zone will eventually result in the depletion of available CAC sorption sites. PFAS concentrations will gradually rise over time in the sorption zone, and may eventually exceed cleanup criteria in groundwater at the downgradient boundary of the CAC sorption zone if the incoming mass flux of PFAS is maintained in the long term. So even if the initial implementation of CAC for PFAS remediation is successful, the question then becomes "How long into the future will this remedy continue to meet remedial action objectives?" The longevity of a CAC remedy is defined as the length of time between the initial CAC injection, and the time when PFAS of interest first exceed applicable regulatory or guidance criteria at the downgradient boundary of the CAC zone.

The authors are not aware of any studies which evaluate the sensitivity of CAC longevity for multiple PFAS with different sorption properties, over a wide range of potential site and remedial design characteristics. Carey et al. (2019) presented a groundwater flow and transport modeling study which indicates that CAC longevity for the remediation of a perfluorooctanesulfonic acid (PFOS) plume at a site in Canada will be on the order of decades, based on site-specific conditions summarized in McGregor (2018).

The purpose of this study is to assess factors that may influence CAC longevity for AFFF-impacted airport sites. Initially, a review of the US Environmental Protection Agency (EPA) and state regulations and guidelines were completed to identify four PFAS of interest upon which to focus this study. A detailed review of a database of PFAS-impacted sites identified the relative concentrations of the four PFAS of interest at 96 AFFF-impacted airport sites. These were later used to justify the source term concentrations for the CAC longevity study. A review of the literature highlighted the impacts of AC particle size and competitive adsorption on breakthrough times. Given the limited experimental and field data related to CAC, several ex situ GAC studies were reviewed to address the similarities and differences one can expect between ex situ GAC treatment and in situ CAC remediation. A review of CAC field applications is presented along with competitive isotherm data generated for the PFAS of interest using a groundwater sample from an AFFF-impacted site. The results of the above reviews were used to formulate a base case simulation that was used to assess CAC longevity at a typical AFFF-contaminated airport site.

2 | PFAS OF INTEREST

When evaluating remedial approaches for PFAS in groundwater, it is important to assess which PFAS are currently of regulatory concern. EPA (2022) issued interim updated drinking water health advisories (HAs) for perfluorooctanoic acid (PFOA) and PFOS of 0.000004 and 0.00002 µg/L, respectively. These HAs replaced the 2016 HAs of 0.07 µg/L for PFOA and PFOS combined that had previously been established by the EPA. These interim HAs are not enforceable and will remain in place until EPA establishes National Primary Drinking Water Regulations. 2022 HAs for PFOA and PFOS are below analytical detection limits (typically on the order of 0.0001–0.001 µg/L), and thus it is uncertain how these are to be implemented in practice. EPA (2022) also issued a final HA for perfluorobutane sulfonate (PFBS) of 2 µg/L. The Agency for Toxic Substances and Disease Registry (ATSDR) has developed federal Minimal Risk Levels (MRLs) for four long-chain PFAAs (ATSDR, 2018): PFOS, perfluorohexanesulfonic acid (PFHxS), PFOA, and perfluorononanoic acid (PFNA). These MRLs are expressed in terms of the oral dose (mg/kg/day), and are also not enforceable. MRLs are developed to assist public health professionals to determine regions and populations potentially at risk for health effects from exposure to a particular chemical.

On the basis of a review of the Interstate Technology and Regulatory Council (2020), 30 of 50 states within the United States have state-specific PFAS criteria. Supporting Information: Table SI.1 lists the number of states with PFAS-specific criteria for each applicable constituent, as well as the median criteria of those that are most relevant to groundwater remediation in applicable states. This table indicates that PFOS and PFOA are the most frequent PFAS constituents with state-specific groundwater criteria (27 of 30 states), with median criteria of 0.07 µg/L. The other two long-chain PFAS constituents with ASTDR risk-based dose limits (PFHxS and PFNA) are the next most common constituents with state-specific criteria (16 and 13 states, respectively), with median criteria of 0.07 and 0.02 µg/L, respectively. PFBS also commonly has state-specific criteria (13 of 30 states), with a criteria range of 0.6–667 µg/L and a median criterion of 5 µg/L. Given the relatively high PFBS state-specific criteria, and the final EPA HA for PFBS of 2 µg/L, this short-chain PFSA is less likely to be of concern at PFAS-impacted sites when compared with the four long-chain PFAAs mentioned earlier. Currently, other short-chain PFAAs are typically not regulated at the federal or state levels, with only a few exceptions as shown in Supporting Information: Table SI.1.

Decisions regarding groundwater remediation at PFAS-impacted sites will depend in part on which PFAS constituents are regulated under applicable state and/or federal regulatory programs. One of

the challenges with PFAS remediation is that because final federal cleanup criteria have not yet been established for PFOS and PFOA, there is some uncertainty about which other PFAAs may be regulated in the future, in addition to analytical challenges at these low concentrations. It is likely that PFOS and PFOA will be the most frequently regulated PFAS for the foreseeable future. It is also reasonable to expect that PFHxS and PFNA will be the next most frequently regulated long-chain compounds of concern, at least at the state level. These four long-chain compounds will be referred to as the PFAS of interest herein.

2.1 | PFAS of interest concentrations at AFFF-impacted sites

A database of PFAS of interest concentrations at AFFF-impacted airport sites was compiled to support the modeling sensitivity analysis presented herein. The Social Science Environmental Health Research Institute (SSEHRI) at Northeastern University has compiled a large list of maximum PFAS concentrations at sites across the United States. This large list (1244 sites based on the December 20, 2020, version of the SSEHRI database) was reviewed to filter a subset of entries that represent AFFF-impacted military and/or civilian airport sites. There are 96 sites listed in the filtered subset of AFFF-impacted airport sites (see Supporting Information: Table SI.2). The maximum concentrations of the PFAS of interest (PFOS, PFHxS, PFOA, and PFNA) are listed in Supporting Information: Table SI.3.

The ranked ratio of PFOS + PFHxS to PFOS + PFHxS + PFOA + PFNA (i.e., total PFAS of interest) is shown in Supporting Information: Figure SI.1. Ninety-five percent of the AFFF-impacted airport sites have higher PFSA concentrations relative to PFCAs for these four PFAS of interest. Eighty-two percent of these sites have PFOS and PFHxS concentrations that were greater than 70% of the sum of these four PFAS of interest. These are relevant statistics with respect to the potential implementation of CAC for in situ remediation at these types of airport sites because PFSAs have a higher affinity to CAC than PFCAs. That said, it is still important to analyze the CAC longevity for PFCAs at these sites because that may be the limiting metric that drives the performance of this type of remedial technology.

The median site maximum concentrations of these four PFAS of interest are 37, 22, 7, and 0.2 μg/L, respectively. Figure 1 shows a box plot with the minimum, 25% quartile, median, 75% quartile, and maximum concentrations based on the site PFAS concentrations listed in Supporting Information: Table SI.3. Figure 1 indicates that PFOS typically has the highest concentrations at AFFF-impacted airport sites, followed closely by PFHxS, then PFOA with concentrations typically about 20%–50% of PFOS and PFHxS concentrations at these sites. PFNA typically has concentrations that are 20–40 times lower than PFOA. Since PFNA has a longer fluorocarbon chain length than PFOA, it should have a higher affinity for sorption to CAC than PFOA. Therefore, the longevity of CAC for PFNA sorption will be longer than PFOA, and will not be evaluated further as part of this study.

3 | LITERATURE REVIEW

3.1 | Freundlich isotherms

The Freundlich isotherm is generally representative of PFAS adsorption to activated carbon because it allows for multilayer sorption which is expected to occur with PFAS, and it represents heterogeneous surface energy on the activated carbon (Du et al., 2014; Q. Yu et al., 2009; Zhang et al., 2016). The Freundlich isotherm is represented using

$$S = K_f C_w^a, \quad (1)$$

where S is the sorbed concentration (mg/kg), K_f is the Freundlich sorption coefficient (mg/kg [mg/L]$^{-a}$), C_w represents the equilibrium aqueous concentration (mg/L), and a is the exponent in the Freundlich isotherm.

For an in situ CAC remedy, the retardation coefficient for sorbing contaminants is calculated using

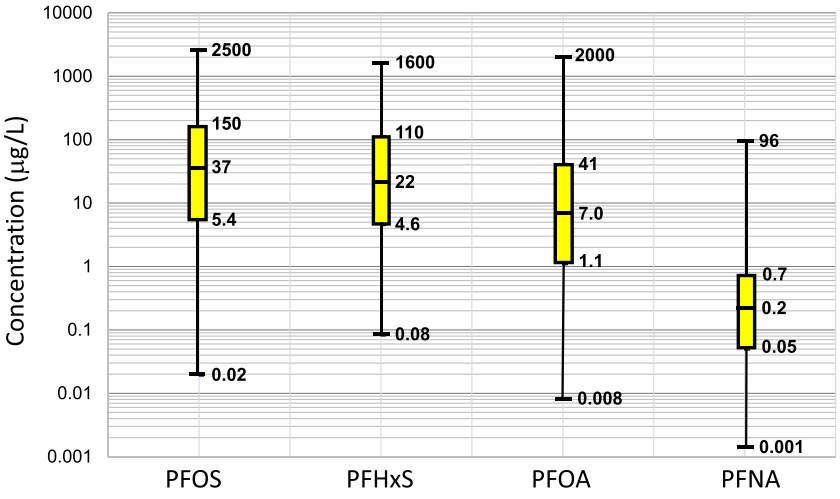

FIGURE 1 Statistical distribution of maximum PFOS, PFHxS, PFOA, and PFNA concentrations measured in groundwater at 96 AFFF-impacted airport sites. Statistics represent the minimum, 25% quartile, median, 75% quartile, and maximum concentrations for the 96 sites in the database. AFFF, aqueous film-forming foam; PFHxS, perfluorohexanesulfonic acid; PFNA, perfluorononanoic acid; PFOA, perfluorooctanoic acid; PFOS, perfluorooctanesulfonic acid.

$$R = 1 + \frac{\rho_b}{\theta}\left(K_f f_{cac} a C_w^{a-1}\right), \quad (2)$$

where R is the retardation coefficient based on sorption to CAC in soil, θ is effective porosity (m^3/m^3), ρ_b is the soil dry bulk density (g/ml), and f_{cac} is the fraction of CAC (g/g).

When comparing isotherms from different batch tests (e.g., single species vs. multiple species isotherms), it is important to review the effects of competitive sorption on both K_f and a since each may change when experimental conditions are varied. Only when a is similar between different experiments can the K_f values be compared to provide a sense of which condition results in higher adsorption. There can also be some confusion in the literature about the values determined for the Freundlich isotherm exponent (a). Some studies use n in place of a in Equation (1), and other studies use $1/n$. When isotherm values are reported in these studies for n, it is important to establish whether the Freundlich exponent (a) is equal to n or $1/n$.

Supporting Information: Table SI.4 presents a summary of 14 studies that have involved the determination of the Freundlich isotherm parameters for PFAS adsorption to coal-based GAC, powdered activated carbon(PAC), and/or CAC, including this current study (Cantoni et al., 2021; Carey et al., 2019; Chularueangaksorn et al.,2014; Hansen et al., 2010; Liu et al., 2020; Ochoa-Herrera & Sierra-Alvarez, 2008; Qu et al., 2009; Siriwardena et al., 2019; J. Yu & Hu, 2011; Q. Yu et al., 2009; Zhang et al., 2021, 2016; Zhi & Liu, 2015). Supporting Information: Table SI.5 includes a description of which sorbent was used in the batch tests, what type(s) of aqueous solutions were used, dissolved organic carbon (DOC) concentrations (if applicable), whether the study included a comparison of GAC and PAC results, whether the batch tests were based on a groundwater sample from the field, whether isotherm results were compared for PFAAs with different fluorocarbon chain lengths, and whether the batch test(s) involved a mixture of multiple PFAAs. Supporting Information: Table SI.5 presents the Freundlich isotherm parameters determined for applicable PFAAs. All K_f values in Supporting Information: Table SI.5 have been normalized to one set of consistent units $(mg/kg\ [mg/L])^{-a}$.

Various results from these isotherm studies are discussed in the following sections to provide insight into expected behavior for PFAS adsorption to CAC based on prior studies of PFAS adsorption to GAC and PAC (only one prior isotherm study for PFAS adsorption to CAC was available at the time that this manuscript was prepared).

3.2 | Activated carbon particle size

GAC particles typically range in size from 500 to 1000 μm, PAC particles from 25 to 100 μm, and CAC particles range up to 1–2 μm. Supporting Information: Figure SI.2 compares the relative scale of GAC, PAC, and CAC particles. GAC particles have high intraparticle porosity which is distributed between micropores (<0.002 μm), mesopores (0.002–0.05 μm), and macropores (>0.05 μm). Siriwardena et al. (2019) state that the length of PFOS and PFOA molecules is about 1 nm, and the diameters are about 0.4 nm. Due to their molecular size, PFOS and PFOA are believed to adsorb more often in mesopores than micropores (<2 nm) as are other long-chain PFAS, whereas short-chain PFAAs may be more dominantly adsorbed in micropores of the activated carbon (Cantoni et al., 2021; Du et al., 2014; Siriwardena et al., 2019; Q. Yu et al., 2009). Du et al. (2014) cite several studies which indicate that activated carbon with a higher proportion of meso- and macropores had a higher sorption capacity for PFOS and PFOA. Du et al. (2014) attribute this partly to micropore blockage, and also due to the larger pore sizes being able to accumulate long-chain PFAS with the potential for aggregation as PFAS concentrations increase. Park et al. (2020) found that GAC with higher micropore surface areas exhibited higher adsorption capacity for hydrophilic and marginally hydrophobic PFAS, and mesopore adsorption was more important for hydrophobic PFAS possibly due to less pore blockage.

There has been significant interest in the use of GAC and PAC for ex situ treatment of PFAS (Qu et al., 2009). CAC is more readily injected into the subsurface at low pressures than PAC and thus has a more uniform distribution after injection (McGregor, 2020b). Hydraulic fracturing would be required to inject PAC or GAC directly into the subsurface because the activated carbon particle size is larger than typical pore spaces in the subsurface. This would cause the formation of preferential pathways, resulting in a high degree of heterogeneity with respect to activated carbon distribution in situ. The goal with activated carbon injections is to try to minimize the degree of distribution heterogeneity within the sorption zone, and to minimize opportunities for groundwater to bypass injected activated carbon.

Xiao et al. (2017) studied the influence of activated carbon particle size on a single-point linear K_d isotherm. Figure 2 illustrates results from Xiao et al. (2017) which indicate that the PFOS K_d is inversely proportional to activated carbon particle size (d_{AC}) oversizes that range from PAC to GAC. This figure is based on 20-day batch tests. While some of the difference between GAC and PAC K_d results may be due to nonequilibrium sorption in the GAC tests, data presented by Xiao et al. (2017) indicate that the overall trend of K_d versus particle size is representative. The variation in pore size distribution between PAC and GAC may be a contributing factor to this trend (Q. Yu et al., 2009). Q. Yu et al. (2009) determined that there was a larger volume of micropores in PAC relative to GAC. Q. Yu et al. (2009) also suggest that higher PFOS and PFOA sorption to PAC relative to GAC may be related to a larger number of surface functional groups on PAC and that more active sorption sites are exposed on the surface of PAC versus GAC. Hansen et al. (2010) suggest that PAC may have a higher adsorption capacity than GAC because the surface area is more accessible on the smaller particle, and PAC may be less prone to fouling through pore throat clogging by native organic matter (NOM).

The difference in sorption affinity for PFAS to CAC versus PAC is uncertain. Bakkaloglu et al. (2021) observed that CAC had a smaller specific surface area, but higher proportions of mesopores and macropores, relative to PAC. This may favor PFOS and PFOA adsorption because these molecules are large compared to micropores. Murray et al. (2019) observed that PFAS adsorption capacity

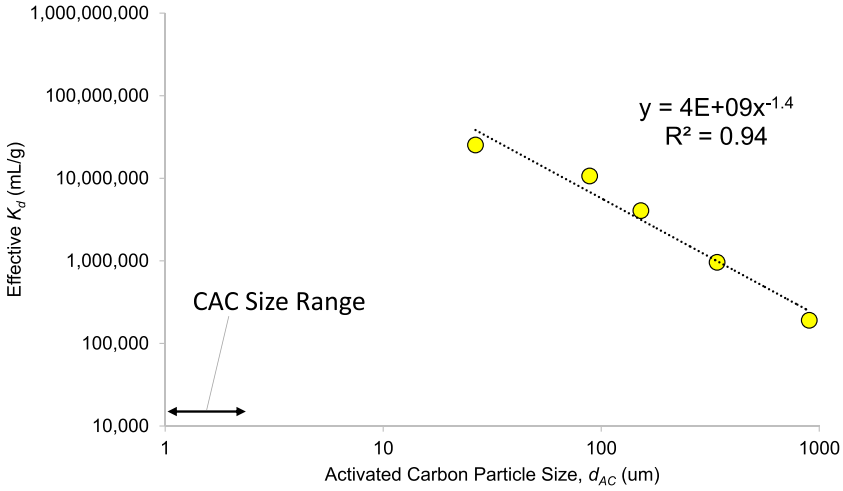

FIGURE 2 Particle size influence on PFOS effective K_d based on 20-day equilibration experimental data presented by Xiao et al. (2017). Experiments were conducted by Xiao et al. (2017) using a groundwater sample from an AFFF-impacted site, with a PFOS concentration of 33 µg/L, and a DOC concentration of 46 mg/L. CAC, colloidal activated carbon; DOC, dissolved organic carbon; PFOS, perfluorooctanesulfonic acid.

with CAC was significantly higher than for GAC, in part because CAC has a greater fraction of meso-/macropores than GAC. The main advantage of CAC is that it is more readily injected into porous media than PAC (McGregor, 2020b), and thus it is the most likely size of activated carbon to be employed for in situ remediation at PFAS sites.

3.3 | Sorption affinity for PFSAs versus PFCAs and influence of fluorocarbon chain length

Numerous studies have found PFSAs have higher sorption affinity with GAC and PAC than PFCAs with similar fluorocarbon chain length, which has been attributed to the sulfonate functional group having a higher degree of hydrophobicity relative to the carboxylate functional group (Hansen et al., 2010; Ochoa-Herrera & Sierra-Alvarez, 2008; Siriwardena et al., 2019). Prior studies have also demonstrated that the relative sorption affinity for PFAAs with GAC and PAC is proportional to the fluorocarbon chain length (Xiao et al., 2017). For example, Supporting Information: Figure SI.3 shows the regression of effective K_d versus fluorocarbon chain length based on results presented in Xiao et al. (2017) for single-point batch tests with a groundwater sample and GAC (Filtrasorb400® or F400). Comparison of single species isotherm for 4- and 8-fluorocarbon chain length PFAAs, as determined by Ochoa-Herrera and Sierra-Alvarez (2008) and Zhang et al. (2021) and summarized in Supporting Information: Table SI.5, demonstrates this same hierarchy. Supporting Information: Figure SI.3 illustrates that PFSAs exhibit a larger influence of fluorocarbon chain length on K_d in the Xiao et al. (2017) study, relative to PFCAs. In other words, there is a larger difference in K_d between short-chain and long-chain PFSAs than for PFCAs.

3.4 | Competitive sorption effects

Implementation of an in situ CAC remedy at PFAS sites involves the establishment of a sorption zone where a suite of chemicals is copresent with PFAS of interest, potentially resulting in competitive inhibition of the adsorption of the PFAS of interest. The main concern with competitive sorption effects is the presence of DOC. For example, J. Yu and Hu (2011) found that the presence of wastewater treatment effluent organic matter at a concentration of 10.2 mg/L resulted in a significant reduction of PFOS and PFOA sorption to PAC. Another study by Siriwardena et al. (2019) did not observe significant competitive inhibition of PFAS sorption to GAC when DOC was present at between 0.1 and 1 mg/L. Carey et al. (2019) presented PFOS single species and groundwater sample isotherms for sorption to CAC, where the groundwater sample included 23.8 mg/L DOC. As discussed later in this study, the presence of DOC at this high concentration in the groundwater sample may have partly contributed to significantly lower PFOS sorption to CAC in the groundwater sample isotherm; however, the authors are not able to quantify the degree of competitive inhibition that occurred between DOC and PFOS during the batch tests.

Due to the relatively large hydrophobicity of some polyfluorinated compounds in source areas at AFFF-impacted sites, including precursors to PFSAs and PFCAs (Houtz et al., 2013), these compounds may competitively inhibit the adsorption of PFAS of interest. Studies that quantify the effect of precursor presence on PFAA sorption isotherms were not found in the literature. As discussed later, one alternative for remediation based on in situ CAC sorption zone is to establish the sorption zone some distance downgradient of the source area, where PFAS precursors are largely attenuated out of groundwater due to adsorption, biodegradation, and/or diffusion into clay/silt along the flow path. This would remove or reduce one source of potential competition for the sorption of PFAS of interest to CAC, because higher molecular weight precursors may compete with PFAAs for sorption sites.

Siriwardena et al. (2019) demonstrated that a solution mixture with PFOS and PFOA and GAC will cause some competitive inhibition of each individual PFAS species, relative to single species solutions for PFOS and PFOA (see isotherms summarized in Supporting Information: Table SI.5). Supporting Information: Figure SI.4 compares the single species and mixture isotherms for

these two species. It is apparent that combining PFOS and PFOA resulted in a decrease in the extent of PFOA sorption to GAC by about a factor of 2, and the effect on PFOS sorption was less than for PFOA.

4 | PFAS BREAKTHROUGH TIMES IN GAC VERSUS CAC

Bench- and full-scale GAC experiments have demonstrated that short-chain PFAAs breakthrough more quickly than long-chain PFAS of interest such as PFOS, PFHxS, and PFOA (Appleman et al., 2014; McCleaf et al., 2017; Franke et al., 2017; Belkouteb et al., 2020; Park et al., 2020). Some of this early breakthrough has been attributed to competitive sorption effects, where long-chain PFAAs and/or natural organic matter (NOM) loading result in the desorption of short-chain PFAAs such as PFBS and/or perfluorobutanoic acid (PFBA; Appleman et al., 2014; McCleaf et al., 2017). This desorption is sometimes evidenced by what is referred to as "over-shoot concentration" (Park et al., 2020), which indicates that the effluent concentration is higher than the influent concentration.

To compare these PFAA breakthrough trends in GAC systems quantitatively, we compiled the original study data (influent and effluent concentrations for Utility 20) for Appleman et al. (2014), McCleaf et al. (2017), and Franke et al. (2017). Utility 20 was the main case study highlighted in Appleman et al. (2014), and it represents a 657-day study conducted with PFAS influent in a full-scale GAC pair of lead and lag vessels. The lead vessel was 2.7 m long, and the combined lead + lag vessel had a length of 5.4 m. McCleaf et al. (2017) present the results of a bench-scale GAC experiment with a reactor vessel length of approximately 0.1 m. Franke et al. (2017) presented the results of a full-scale GAC study with an unknown reactor vessel length.

The McCleaf et al. (2017) data were obtained from Englund (2015), Lindegren (2015), and Ostlund (2015) for the 217-day bench-scale experiment. The GAC results were normalized by using the same removal efficiency calculation presented in McCleaf et al. (2017) for all three experiments. To facilitate a comparison with potential breakthroughs for in situ CAC sorption zones, the GAC experiments were normalized by using pore volumes instead of bed volumes which are more typically reported for GAC studies. To estimate pore volumes, an interparticle porosity of 0.4 was assumed for the three GAC experiments and it was assumed that intraparticle groundwater flow was negligible. The McCleaf et al. (2017) experiment removal efficiency calculations were further modified by using the influent concentrations that were measured on the same day as effluent concentrations. McCleaf et al. (2017) calculated an average influent concentration over the entire experimental period, but due to significant fluctuations in some PFAS influent concentrations over time, this resulted in potential artifacts in removal efficiency trends over part of the experimental period. For example, there was a sharp reduction in influent concentrations for a number of PFAS at around Day 46 in the experiment, followed by a significant increase to a more stable influent concentration at around Day 91. This decrease in influent concentration would have resulted in some desorption in the GAC vessel, so the calculated removal efficiencies between Days 46 and 91 were not used in this current study.

Figure 3 presents the modified removal efficiency versus pore volume data based on the McCleaf et al. (2017) study data for PFCAs, and Supporting Information: Figure SI.5 presents the removal efficiency versus pore volume data for PFSAs. In general, the removal efficiency is shown to be declining exponentially over time in Figure 3 based on the regression analysis. The reason for this exponential decline trend is uncertain; it may be due at least in part to declining sorption affinity as a result of increasing competitive sorption effects due to the loading of other sorbates over time. Two PFCAs show some evidence of desorption due to competitive inhibition: PFBA, which has effluent concentrations up to 12% more than influent concentrations at one point in the experiment; and perfluoropentanoic acid (PFPeA), which has effluent concentrations up to 13% higher than the influent level. The other PFCAs exhibit slower rates of decline in removal efficiency over time relative to PFBA and PFPeA and do not have effluent concentrations higher than influent levels (negative removal efficiency). It is uncertain the extent to which these declining removal efficiency trends are due to competitive inhibition, as opposed to lower degrees of hydrophobicity associated with lower fluorocarbon chain length as shown in Supporting Information: Figure SI.3. There is clearly some desorption of PFBA occurring in the GAC reactor vessel, but it may be a relatively small amount, and not all of the PFBA decline in removal efficiency can be confirmed to be due to competitive inhibition.

Figure 4 compares the regression of the PFHxS removal efficiency decline rate for the McCleaf et al. (2017) bench-scale system (vessel length of 0.1 m), with the full-scale GAC removal rate observed in Franke et al. (2017). The exponential decline rates are similar for these two different systems which had different vessel lengths. Additional research is needed to understand what factors may influence the removal efficiency decline rate in GAC systems.

The lag period shown in Figure 4 represents the time between the start of the experiment and when a PFAS constituent is first detected. As shown in Figure 4, there is a lag period of about 15,000 pore volumes before PFHxS is detected in the effluent of the full-scale GAC study (Franke et al., 2017). Yet there is no observable lag period for PFHxS to be detected in the McCleaf et al. (2017) bench-scale column with a GAC bed length of 0.1 m.

The lag period (i.e., time before the first detection in the effluent) is directly proportional to the length of the reactor vessel, as shown in Figure 5. Figure 5 also demonstrates that the lag period exhibits the same hierarchy for PFSAs versus PFCAs, and dependence on fluorocarbon chain length, as observed for sorption affinity with GAC. That is, PFOS has a longer lag period than PFOA, and PFOA has longer lag periods than perfluorohexanoic acid and PFBA based on these three GAC experiments.

Figure 6 presents the removal efficiency half-life versus the fluorocarbon chain length, and it distinguishes between trends for PFSAs versus PFCAs. This figure demonstrates that the removal

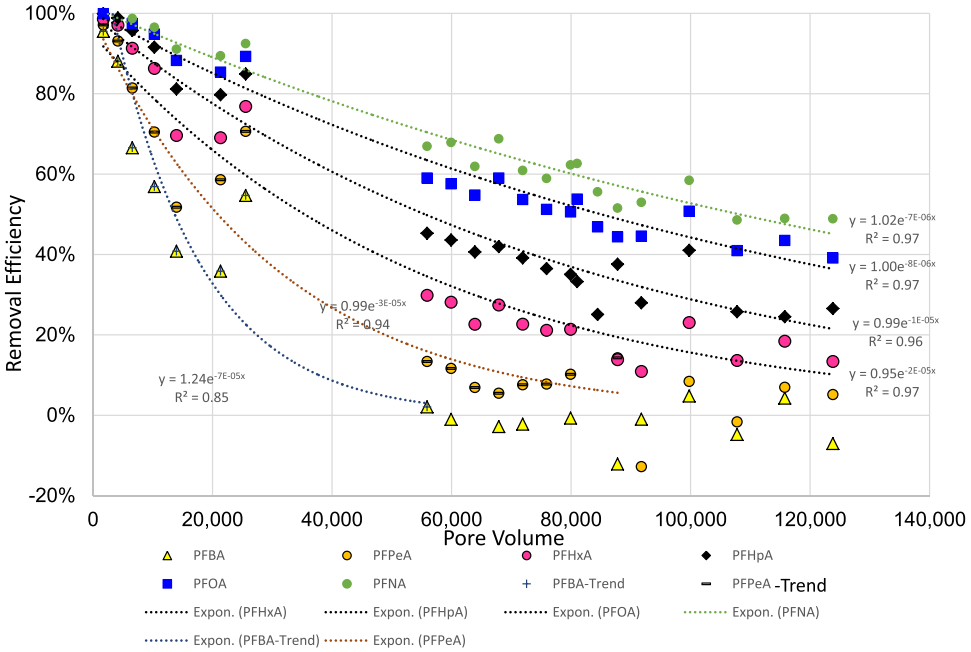

FIGURE 3 Modified GAC bench-scale removal efficiency versus pore volume for PFCAs, based on data originally presented in McCleaf et al. (2017), Englund (2015), Lindegren (2015), and Ostlund (2015). Regression was used to estimate the average rate of removal efficiency decline using a first-order exponential rate model. PFBA and PFPeA removal efficiencies less than zero were not used in the regression analysis. PFBA-trend and PFPeA-trend represent data used for the regression analysis. GAC, granular activated carbon; PFBA, perfluorobutanoic acid; PFCA, perfluorocarboxylate; PFHpA, perfluoroheptanoic acid; PFHxA, perfluorohexanesulfonic acid; PFNA, perfluorononanoic acid; PFOA, perfluorooctanoic acid; PFPeA, perfluoropentanoic acid.

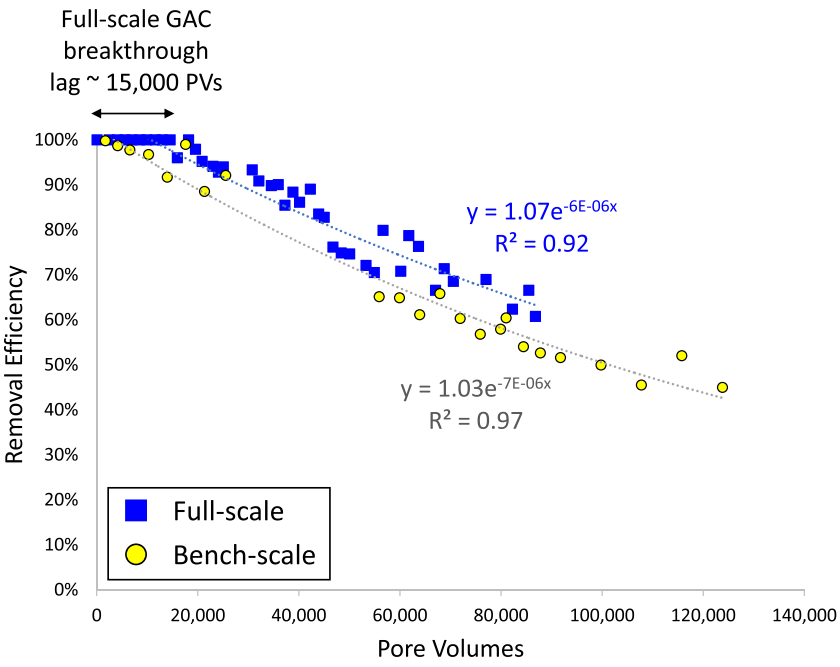

FIGURE 4 Comparison of PFHxS removal efficiency trends for bench-scale (McCleaf et al., 2017) and full-scale (Franke et al., 2017) GAC studies. Pore volume represents the number of pore volumes flushed through the GAC bed. Pore volume calculations are based on an interparticle porosity of 0.4. GAC, granular activated carbon; PFHxS, perfluorohexanesulfonic acid; PV, photovoltaic.

efficiency declines more slowly for PFSAs relative to PFCAs. These trends for GAC removal efficiency declines raise the question of whether similar trends will be observed for PFAAs with in situ CAC remediation. On the basis of the dependence of sorption affinity with fluorocarbon length noted in the above studies, it is expected that short-chain PFAAs will breakthrough (and thus have shorter longevity) in CAC sorption zones relative to long-chain PFAAs, similar to the GAC studies described above.

There are notable differences, however, between the prior GAC studies and in situ CAC applications, including:

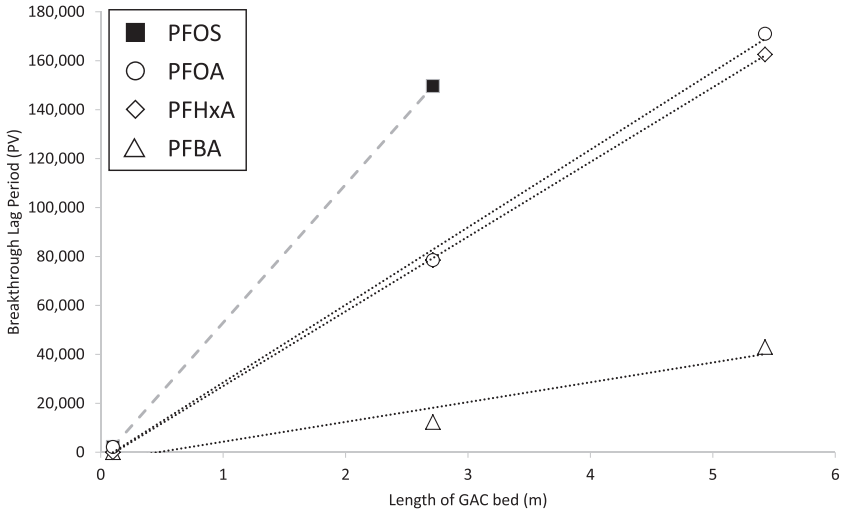

FIGURE 5 Breakthrough lag period versus length of GAC bed. Data for the shortest GAC bed length of 0.1 m are based on McCleaf et al. (2017), and data for the longer GAC bed lengths are based on the study at Utility 20 presented in Appleman et al. (2014) including results for the lead and lag GAC vessels. GAC, granular activated carbon; PFBA, perfluorobutanoic acid; PFHxA, perfluorohexanesulfonic acid; PFOA, perfluorooctanoic acid; PFOS, perfluorooctanesulfonic acid.

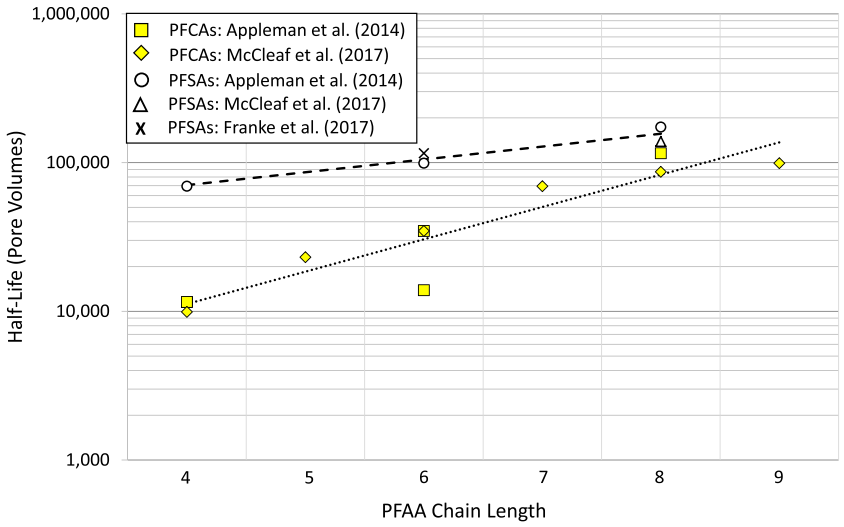

FIGURE 6 Removal efficiency decline half-life versus molecular chain length for PFCAs and PFSAs. PFAA, perfluoroalkyl acid; PFCA, perfluorocarboxylates; PFSA, perfluorosulfonates.

- Average linear groundwater velocity—GAC velocities for Appleman et al. (2014) and McCleaf et al. (2017) were calculated to be 185,000 and 22,000 m/year, respectively. When compared to the 60th percentile groundwater velocity of 19 m/year at 400 contaminated sites as cited in Seyedabbasi et al. (2010); the bench-scale and full-scale GAC systems had a velocity that was on the order of 1000–10,000 times faster than would be present in an in situ CAC system at the majority of contaminated sites. The rapid velocity in GAC systems, where retention times are measured on the order of minutes, means that adsorption kinetics and diffusion limitations may play a large role in GAC breakthrough curves, whereas these are not expected to be a factor for in situ CAC sorption zones where velocity is much slower. As an example of the influence that velocity may have on GAC removal efficiency, Belkouteb et al. (2020) observed increases in PFAS removal efficiency between 6.5% and 14% when the flow rate was decreased by approximately 25%.
- When breakthrough is calculated with respect to pore volumes, the actual breakthrough of short-chain PFAAs is expected to occur more slowly in time for in situ CAC sorption zones, based on a simple comparison to GAC systems, because the retention time for in situ CAC sorption zones are orders of magnitude longer than for the ex situ GAC systems where breakthrough has been observed.

For the reasons stated above, it is difficult to draw quantitative parallels between the observations in these GAC systems and what one might expect for in situ CAC systems. Qualitatively, however, the faster breakthrough of short-chain PFAS, and faster breakthrough of PFCAs relative to PFSAs having the same number of perfluorocarbon chain lengths, is expected.

5 | REVIEW OF CAC FIELD STUDIES

Equation (2) indicates that the retardation coefficient describing PFAS sorption to CAC is directly proportional to f_{cac}. This is a remedial design parameter that can be at least partially controlled by adjusting the CAC dose in the injected solution. Increasing f_{cac} in situ

will result in a larger retardation coefficient and greater remedy longevity.

McGregor (2018) describes the first field-scale application of CAC for the in situ remediation of PFAS worldwide. Since that time, at least 16 other sites have had pilot- or full-scale CAC injections at PFAS sites in the United States, Canada, the United Kingdom, and Saudi Arabia. Table 1a presents a summary of site characteristics and monitoring results for four of these sites (Field Sites 1–4) where the average f_{cac} was measured after the injection of CAC. These four sites are described in McGregor (2018), Carey et al. (2019), McGregor (2020a), McGregor and Benevenuto (2021), and McGregor and Zhao (2021). Table 1a includes descriptions of maximum PFAS concentrations observed within or upgradient of the area where CAC was injected at each site; types and maximum concentrations of organic co-contaminants; soil type; description of the monitoring well network; and the number, times, and description of post-CAC injection monitoring events. Table 1b presents a summary of similar characteristics for 13 sites where f_{cac} was calculated before injection based on

$$f_{cac} = C_w P_{filled} \theta / \rho_b, \quad (3)$$

where P_{filled} represents the ratio of the injected solution volume to the effective pore space volume within the sorption zone where CAC is to be injected.

All 17 field sites listed in Table 1a,b involved the injection of PlumeStop™ CAC. Table 1a,b only include references to CAC injections into unconsolidated media, which is the focus of this current study. Examples of CAC implementation in fractured bedrock are described by McGregor and Benevenuto (2021) and REGENESIS (2022).

Of the 17 sites listed in Table 1a,b, 16 of these sites had maximum concentrations specified for individual PFAS constituents before CAC injection, including PFOS and PFOA. One site has only a maximum total PFAS concentration specified (Field Site 10 in Table 1b) at 1.673 µ/L. PFOS was detected at 14 of 16 sites, with maximum concentrations ranging from 0.008 to 152 µg/L upgradient of the CAC sorption zone, and a median concentration of 1.02 µg/L. PFOA was also detected at 14 sites, with maximum concentrations ranging from 0.042 to 29.2 µg/L, and a median maximum site concentration of 0.897 µg/L. This demonstrates that on average, CAC has been implemented at sites with concentrations in the 1 µg/L range, although CAC has been implemented at some sites with significantly higher concentrations.

As shown in Table 1a,b, CAC remedies have been implemented for PFAS in a wide range of lithologies, with the most common applications to date occurring in silty sand and fine sand aquifers (13 of 17 sites). McGregor (2018, 2020a), McGregor and Benevenuto (2021), and McGregor and Zhao (2021) demonstrate that f_{cac} measured after CAC injection has relatively narrow ranges within each of the four respective injection zones, with average f_{cac} measurements of 0.02%, 0.08%, 0.76%, and 0.07%, respectively. McGregor (2020b) attributes the successful widespread distribution of CAC in situ to the low-pressure injections that may be achieved as a result of the small particle size of CAC.

McGregor (2020b) demonstrated that trying to inject PAC was not as successful because higher injection pressures were required, resulting in preferential PAC distribution in more permeable lenses of sand. McGregor (2020b) also observed preferential accumulation of PAC within the sand packs of monitoring wells that were present at the time of injection at four sites, whereas CAC accumulation was observed not to have occurred in these same monitoring wells. The number of postinjection monitoring events at these 17 field sites ranged from 1 to 12, with a median of 5 monitoring events after CAC injection. Maximum monitoring periods at these sites ranged from 0.3 to 6 years, with a median of 1.2 years. Where identified, PFAS detection limits varied between sites for target constituents (typically PFOS and PFOA), and ranged as high as 0.01 µg/L at Field Sites 1 and 8. PFAS monitoring results at these 17 sites may be characterized as follows:

- PFAS concentrations were reduced below or close to detection limits, or below target criteria at nine sites based on the most recent monitoring results (Field Sites 1, 2, 3, 4, 5, 6, 7, 8, and 17). Five of these nine sites had available data to indicate that this level of the reduction applies to both short- and long-chain PFAAs. Four of the nine sites only had available data for PFOS and PFOA.
- Overall PFAS concentrations are characterized as having been reduced by >90%–99% at four other sites, where individual PFAS concentrations are not available (Field Sites 11, 13, 14, and 15).
- Field Site 12 had reductions in PFOS, PFHxS, PFOA, and PFNA concentrations of >99%, >98%, >99%, and >99%, respectively, after 0.3 years of monitoring.
- Field Site 9 had PFAS reductions ranging from 82% to >99%, which suggests that downgradient monitoring wells are capturing groundwater from zones with differing f_{cac} (assuming that co-contaminant and geochemical conditions are similar at all downgradient wells).
- Field Site 10 (landfill site) had an initial reduction in PFAS concentrations of 91%, but then PFAS concentrations were later observed to increase due to ongoing loading of high DOC in groundwater (greater than 20 mg/L) from landfill leachate.
- Field Site 16 is waiting for analytical results to come in from the first round of groundwater monitoring after the CAC injection.

These results indicate that CAC was successful at reducing PFAS concentrations by >90% to >99% at 14 of 16 sites with available data. All four sites listed in Table 1a, where f_{cac} was measured to be distributed relatively uniformly at each site after injection, had concentrations of both short- and long-chain PFAS reduced below or close to detection limits over the entire monitoring period (from 1 to 6 years). Before the new EPA HAs, these results with PFAS slightly above or below detection limits would have been sufficient. Now, however, the federal HAs are below detection limits (which is not

TABLE 1a CAC field studies with a measured fraction of CAC in soil (f_{cac})

Field site ID	Reference	Maximum detected PFAS groundwater concentrations before CAC injection(μg/L)	Maximum concentrations of co-contaminants before CAC injection (μg/L)	Soil type	Measuredf_{cac}	Description of monitoring network within the CAC adsorption zone	No. of postinjection monitoring events	Postinjectionmonitoring events (days after injection)	Summary of postinjection PFAS monitoring results
1	McGregor (2018), Carey et al. (2019)	PFOA: 3.26 and PFOS: 1.45	BTEX: 300 GRO: 2000 DRO: 3500	Silty sand	0.02%	Four monitoring wells	11	79, 175, 298, 350, 449, 533, 689, 1050, 1415, 1780, 2145	No detections of PFAS in the CAC adsorption zone over first 10 postinjection monitoring events (5 years), with the exception of a single well with low detections of PFOS and PFUnA at t = 533 days (40 and 20 ng/L, respectively). First five monitoring events included lab analysis for only PFOS and PFOA; lab analysis in the last six events included a full suite of PFAAs. In Event 11 (6 years), the detection limits were lowered to about 1 ng/L, and several PFAS were observed slightly above the new detection limits in this last event.
2	McGregor, 2020a	PFBA: 6.2; PFPeA: 24.0; PFHxA: 16.1; PFHpA: 6.08; PFOA: 0.45; and PFNA: 0.14	Petroleum hydrocarbons: 3500	Fine-grained sand	0.08%	Three monitoring wells and one well multilevel with three screened intervals	5	92, 184, 278, 366, 549	No detections of PFAS in the CAC adsorption zone over all five postinjection monitoring events (1.5 years).
3	McGregor and Benevenuto (2021)	PFBA: 6.405; PFPeA: 24.0; PFHxA: 15.74; PFHpA: 7.25; PFOA: 0.91; PFNA: 0.165; and PFOS: 2.105	Total BTEX: 6160	Silty sand and sand	0.76%	Three multilevel wells (two wells with seven screened intervals, and one well with three screened intervals)	3	182, 273, 366	No detections of PFAS in the CAC adsorption zone in unconsolidated media over all three postinjection monitoring events (1 year).
4	McGregor and Zhao (2021)	PFBA: 0.795; PFPeA: 12.8; PFHxA: 3.24; PFOA: 0.95; and PFOS: 2.14	TCE: 985 *cis*-1,2-DCE: 258 vinyl chloride: 54	Silty sand	0.07%	Three monitoring wells	5	122, 248, 362, 547, 724	No detections of PFAS in the CAC adsorption zone over all five postinjection monitoring events (2 years).

Abbreviations: BTEX, benzene, toluene, ethylbenzene, and xylenes; CAC, colloidal activated carbon; DCE, dichloroethene; DRO, diesel range organics; GRO, gasoline range organics; PFAS, per- and polyfluoroalkyl substances; PFBA, perfluorobutanoic acid; PFHpA, perfluoroheptanoic acid; PFHxA, perfluorohexanesulfonic acid; PFNA, perfluorononanoic acid; PFOA, perfluorooctanoic acid; PFOS, perfluorooctanesulfonic acid; PFPeA, perfluoropentanoic acid; PFUnA, perfluoroundecanoic acid; TCE, trichloroethene.

TABLE 1b CAC field studies with a calculated fraction of CAC in soil (f_{cac})

Field site ID	Site name	Maximum detected PFAS groundwater concentrations before CAC injection (μg/L)	Maximum concentrations of co-contaminants before CAC injection (μg/L)	Soil type	Effectiveporosity	Solution volume: Effective pore volume
5	Airport Site #1, UK	PFBA: 1.52; PFPeA: 3.08; PFHpA: 0.64; PFHxA: 2.96; PFOA: 0.316; PFNA: 0.01 PFBS: 0.02; PFPeS: 0.0183; PFHxS: 0.075; PFOS: 0.0142; 6:2 FtS: 27.8	None detected	Silt with fine sand lenses (matrix-dominated unstructured chalk)	0.15	0.7
6	Airport Site #2, UK	PFBA: 5.47; PFPeA: 31.46; PFHxA: 18.02; PFHpA: 5.54; PFOA: 5.66; PFNA: 0.68; PFDA: 0.05; PFDoA: 0.05; PFUnA: 0.05; PFTrDA: 0.05; PFTeDA: 0.05 PFBS: 0.05; PFPeS: 0.05; PFHxS: 0.47; PFHpS: 0.1; PFOS: 0.67; PFNS: 0.05; PFDS: 0.05 4:2 FtS: 0.1; 6:2 FtS: 149.1; 8:2 FtS: 1.62; N-EtFOSAA: 0.2; N-MeFOSAA: 1; PFOSA: 1	PAH 16 - 0.005 Mixed VOCs up to 0.2 (1,2,3-trichlorobenzene) Elevated metals	3.0–5.0 m BGL heterogenous made ground, occasional alluvium; 5.0–8.0 sand and gravel (river terrace deposits)	0.23	0.7
7	Airport Site, AK	PFOA: 0.24; PFOS: 0.28	None detected	Silty Sand	25%	80%
8	Camp Grayling, MI	PFHxS: 0.05; PFOS: 0.06	PCE: 0.01	Silty sand	0.25	0.46
9	HM Refinery, MI	PFOS: 0.5	TPH DRO: 0.5	Silty sand with gravel and clay	0.33	0.7
10	Landfill Pilot Test, PA	Total PFAS: 1.673	None detected	Sandy fill with cobbles, overlying clay, overlying sandy/weathered bedrock	25%	70%
11	Manufacturing Plant, MI	PFBA: 0.437; PFPeA: 0.664; PFHxA: 1.8; PFHpA: 0.243; PFOA: 0.858 PFBS: 1.5; PFHxS: 7.9; PFOS: 3.54	Total chlorinated VOCs: 0.068	Silty sand	0.15	0.8
12	Newport Site, WA	PFOA: 0.14; PFNA: 0.19 PFHxS: 0.39; PFOS: 2.60	None detected	Silty sand	23%	70%
13	Refinery Site, MI	PFOA: 29.2; PFOS: 153	TPH DRO: 1,000	Silty sand with clay	0.23	0.7

(Continues)

TABLE 1b (Continued)

Field site ID	Site name	Maximum detected PFAS groundwater concentrations before CAC injection (μg/L)	Maximum concentrations of co-contaminants before CAC injection (μg/L)	Soil type	Effectiveporosity	Solution volume: Effective pore volume
14	Site #1, NY	PFOA: 5.7; PFOS: 0.008	TCE: 0.13 *cis*-1,2-DCE: 0.008 1,1,1-TCA: 0.019	Sand	25%	39%
15	Site #2, NY	PFOA: 0.884; PFNA: 0.179	TCE: 4.7	Silty sand and clay	20%	72%
16	Site #3, NY	PFBA: 0.18; PFPeA: 0.32; PFHxA: 1.52; PFHpA: 0.119; PFOA: 0.042 PFBS: 0.73; PFHxS: 0.847; PFHpS: 0.031; PFOS: 1.04	None detected	Silty sand	23%	70%
17	USEPA Superfund Site, CT	PFOA: 1 PFOS: 1	BTEX: 0.53 *cis* 1,2-DCE: 0.113 VC: 0.212 1,2,4 -TMB: 0.028	Sand/Gravel	30%	100%

Field site ID	Carboninjection concentration(mg/L)	Estimated f_{cac}	Description of monitoring well network	No. of Postinjection monitoring events	Postinjection monitoring events (days after injection)	Summary of postinjection PFAS monitoring results
5	40,000	0.26%	One well 10 m upgradient; and three wells at 0.75, 5, and 10 m downgradient.	6	41, 88, 116, 152, 178, 230	Reduction of target compounds PFOS/PFOA to below or close to detection limit (0.0003/0.0002 μg/L)
6	25,000	0.25%	Shallow/deep nest at 3.8 m upgradient; shallow/deep nest in the sorption zone; and shallow/deep nest at 5 m downgradient.	7	90, 124, 145, 176, 208, 232, 329	Reduction of target compounds PFOS/PFOA to below or close to detection limit (0.00025/0.005 μg/L)
7	20,950	0.26%	One well	5	47, 321, 386, 482, 542	Nondetect
8	8000	0.06%	Six wells downgradient at distances of 2, 5, 8, and 14 m	7	27, 58, 100, 132, 170, 358, 595	All monitoring wells are ND (<0.01 μg/L)
9	22,000	0.32%	Three wells within the sorption zone	3	104, 227, 619	82% to >99%
10	6000	0.07%	One well upgradient, and two wells downgradient of the sorption zone at distances of 1.5 and 2.4 m	4	48, 85, 107, 218	Organic content too high from landfill leachate, initial postinjection results 91% reduction in total PFAS from 1.673 to 0.150 μg/L, subsequent sampling did not meet Pilot goal, and recommended Organic Content analysis. CAC observed on dedicated well sampling tubing and organic content above 20 mg/L

TABLE 1b (Continued)

Field site ID	Carboninjection concentration(mg/L)	Estimated f_{cac}	Description of monitoring well network	No. of Postinjection monitoring events	Postinjection monitoring events (days after injection)	Summary of postinjection PFAS monitoring results
11	18,000	0.14%	One well within the sorption zone, and two wells at 6 m and 12 m downgradient	7	19, 47, 110, 146, 200, 291, 370	Within the treatment zone, total PFAS reductions have been >92%
12	22,123	0.22%	One well	3	50, 80, 120	PFOA: 0.0011 J; PFOS: 0.011; PFNA: 0.0015 J; PFHxS: 0.0043
13	35,000 and 72,000	0.21%	12 wells within the sorption zone and 12 wells downgradient	4	Ranges by area, but generaly data has been collected monthly, starting 3 months post application.	In 5 of the 12 areas of the site where CAC placement was verified, initial results showed >99% reduction, two areas showed >95% reduction. Areas with marginal placement validation data were reinjected and we are currently awaiting data
14	18,000	0.11%	One well mid-way through the treatment zone and 1 well downgradient	6	30, 60, 120, 210, 365, 730	95%–99% PFAS reduction, TCE removed. Confirmation that reductions continue to be maintained through Q1 2022
15	19,000	0.17%	Two upgradient, two within the treatment zone, and one downgradient	4	32, 67, 102, 129	>90% reductions
16	22,000	0.22%	One well in the treatment zone, and one downgradient	1	290	NYS awarded a certificate of completion groundwater data collected June 2022—waiting for results
17	10,000	0.19%	Four wells immediately downgradient the trench, additional four wells 3 m from the barrier, and additional wells downgradient approximately 15 m. After approximately 1 year the number of wells sampled was reduced to four.	12	7, 21, 41, 69, 97, 107, 142, 205, 292, 657, 1022, 1387	CT state goals met and maintained through latest sampling in target wells

Abbreviations: BTEX, benzene, toluene, ethylbenzene, and xylenes; CAC, colloidal activated carbon; DCE, dichloroethene; DRO, diesel range organics; FtS, fluorotelomer sulfonate; GRO, gasoline range organics; ND, non-detect; N-EtFOSAA, N-ethylperfluorooctanesulfonamidoacetic acid; N-MeFOSAA, N-methylperfluorooctanesulfonamidoacetic acid; PCE, perchloroethylene; PFAS, per- and polyfluoroalkyl substances; PFBA, perfluorobutanoic acid; PFBS, perfluorobutane sulfonate; PFDA, perfluorodecanoic acid; PFDoA, perfluorododecanoic acid; PFHpA, perfluoroheptanoic acid; PFHpS, perfluoroheptanesulfonic acid; PFHxA, perfluorohexanesulfonic acid; PFHxS, perfluorohexanesulfonic acid; PFNA, perfluorononanoic acid; PFOA, perfluorooctanoic acid; PFOS, perfluorooctanesulfonic acid; PFPeA, perfluoropentanoic acid; PFPeS, perfluoropentanesulfonic acid; PFTeDA, perfluorotetradecanoic acid; PFTrDA, perfluorotridecanoic acid; PFUnA, perfluoroundecanoic acid; TCA, 1,1,1-trichloroethane; TCE, trichloroethene; TPH, total petroleum hydrocarbons; USEPA, US Environmental Protection Agency; VC, vinyl chloride; VOC, volatile organic compound.

attainable in practice). While these HAs are not enforceable, it may be necessary to increase the sorption zone length and/or CAC dose if final cleanup goals end up being close to these new HAs. Alternatively, CAC remedies may be employed with the interim goal of mass flux reduction in plumes, in which case having downgradient results only slightly above detection limits would still be qualified as a success.

Inspection of organic co-contaminant concentrations indicates that chlorinated solvent concentrations up to 1000 µg/L and petroleum hydrocarbon concentrations up to 6160 µ/L did not inhibit the initial success of the CAC injections, with respect to PFAS reductions below detection limits (e.g., Field Sites 1–4). These short-term data do not indicate, however, whether these co-contaminant concentrations will influence remedy longevity.

One of the field sites has had monitoring conducted for a period of 6 years, although most sites have had 2 years or less of monitoring conducted. In general, CAC is shown to be successful for short- and long-chain PFAS compounds in the short-term; however, the longevity of this remedy, as well as site-specific factors that govern this longevity, have only been assessed to date by Carey et al. (2019) for a single site.

6 | PFAS–CAC ISOTHERMS FOR AFFF-IMPACTED GROUNDWATER SAMPLE

Isotherms summarized as part of the literature review were based on GAC and PAC batch tests. Carey et al. (2019) present two CAC isotherms: one for PFOS in a single species solution (K_f = 142,800 mg/kg [mg/L]$^{-a}$ and a = 0.59), and one for PFOS based on a groundwater sample collected from an AFFF-impacted airport site (K_f = 4900 mg/kg [mg/L]$^{-a}$ and a = 0.24). Carey et al. (2019) indicate that the groundwater sample had the following concentrations for PFAS of interest: PFOS 208 µg/L, PFHxS 65.6 µg/L, PFOA 20.8 µg/L, and PFNA 0.552 µg/L. Total PFSAs were 281.8 µg/L, total PFCAs were 46.9 µg/L, and total detected precursors were 60.2 µg/L. The detected precursors mainly consisted of 6:2 fluorotelomer sulfonate (6:2 FtS) at 40.4 µg/L, and 8:2 FtS at 17.5 µg/L. The DOC concentration in this groundwater sample was 23.8 mg/L, which is sufficiently high to compete with the PFAS of interest for sorption to CAC. The reduced PFOS sorption affinity to CAC observed in the groundwater sample isotherm, relative to the single species isotherm, reflects competitive sorption between PFOS and other compounds in the groundwater mixture, including NOM, precursors (detected and undetected/unknown), and/or other PFAAs.

Another set of PFAS Freundlich sorption isotherms was developed as part of this current study using different analytical equipment than was utilized in the 2019 study. The adsorption of PFOS, PFHxS, 6:2 FtS, and PFOA onto CAC was investigated in batch mode, employing polypropylene test tubes that contained 50 ml solution. One set of experiments was conducted. The test solution is the AFFF-contaminated groundwater sample described earlier. To initiate the adsorption experiment, different volumes of the CAC stock solution (modified PlumeStop™) were added to each test tube, and the tubes were shaken on an orbital shaker. After 72 h, an aliquot was taken out from each test tube and transferred into a 13-ml ultracentrifuge tube. CAC was separated from the solution by ultracentrifugation at 230,000g for 105 min, and 250 µl of the supernatant was collected for PFAS analysis by liquid chromatography-tandem mass spectrometry. Control (liquid chromatography–mass spectrometry) experiments indicated that the amount of PFAS adsorbed to the polypropylene test tube and ultracentrifuge tube was always less than 10% of the initial concentration. Therefore, the amount of each constituent adsorbed onto CAC was calculated by subtracting the amount that remained in the solution after 72 h from the initial amount, using the following equation:

$$S = \frac{C_0 - C_w}{C_{CAC}}, \tag{4}$$

with C_0 (mg/L) being the initial concentration of PFAS, and C_{CAC} being the concentration of CAC (kg/L).

Freundlich isotherms in this current study were estimated for PFOS (K_f = 12,000 mg/kg [mg/L]$^{-a}$ and a = 0.33), PFHxS (K_f = 1240 mg/kg [mg/L]$^{-a}$ and a = 0.24), PFOA (K_f = 580 mg/kg [mg/L]$^{-a}$ and a= 0.25), and 6:2 FtS (K_f = 3900 mg/kg [mg/L]$^{-a}$ and a = 0.2). Figure 7 compares the isotherms presented by Carey et al. (2019) at a higher polymer concentration, with the isotherms estimated for this current study using a lower polymer concentration. Figure 7 demonstrates that the order of sorption affinity with CAC, based on the solution with the lower polymer concentration, is PFOS > 6:2 FtS > PFHxS > PFOA, which is consistent with the GAC breakthrough timing observed for the three PFAAs in McCleaf et al. (2017) and Belkouteb et al. (2020).

Figure 7 illustrates that at an equilibrium aqueous concentration of 1 µg/L, there is about a 5 times difference in sorption affinity between PFOS and PFHxS for the groundwater sample with the current isotherms, and about 10 times difference between PFOS and PFOA.

7 | MODELING CAC LONGEVITY FOR PFAS IN SITU REMEDIATION

Carey et al. (2019) described a multispecies reactive transport model which has been modified to facilitate the modeling of CAC injection for the purpose of evaluating remedy longevity. The model is referred to as in situ remediation or ISR-MT3DMS. MODFLOW is used to simulate groundwater flow conditions before reactive transport simulations with ISR-MT3DMS. ISR-MT3DMS is typically used to simulate the injection of CAC into an existing PFAS plume. Carey et al. (2019) derived a mass-balance-based equation to calculate the PFAS aqueous concentration immediately after CAC injection and re-equilibration of partitioned concentrations within the CAC sorption zone. The re-equilibration process is assumed to be an instantaneous

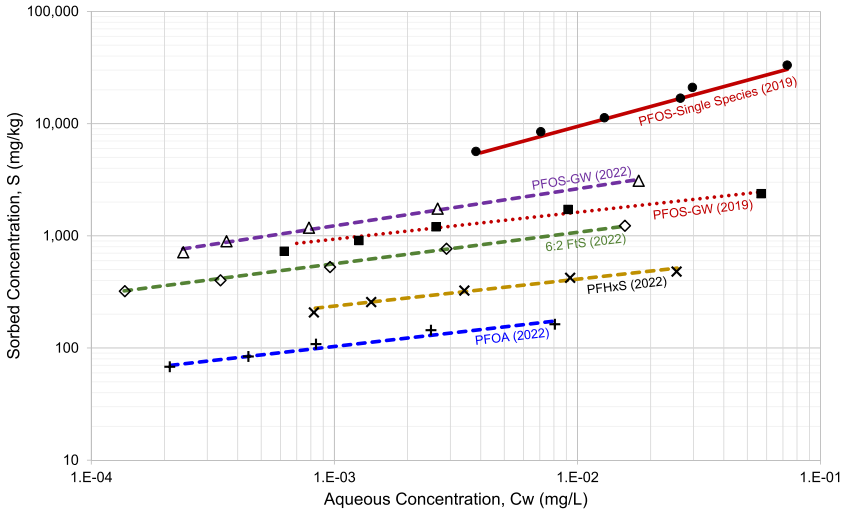

FIGURE 7 Comparison of PFOS, PFHxS, PFOA, and 6:2 FtS isotherms for adsorption to CAC based on Carey et al. (2019) and this study (2022). Two solutions were used: (i) PFOS single species (2019 only); and (ii) groundwater (GW) sample from an AFFF-impacted site (2022). Different analytical equipment was used in the 2019 and 2022 studies. AFFF, aqueous film-forming foam; CAC, colloidal activated carbon; FtS, fluorotelomer sulfonate; PFHxS, perfluorohexanesulfonic acid; PFOA, perfluorooctanoic acid; PFOS, perfluorooctanesulfonic acid.

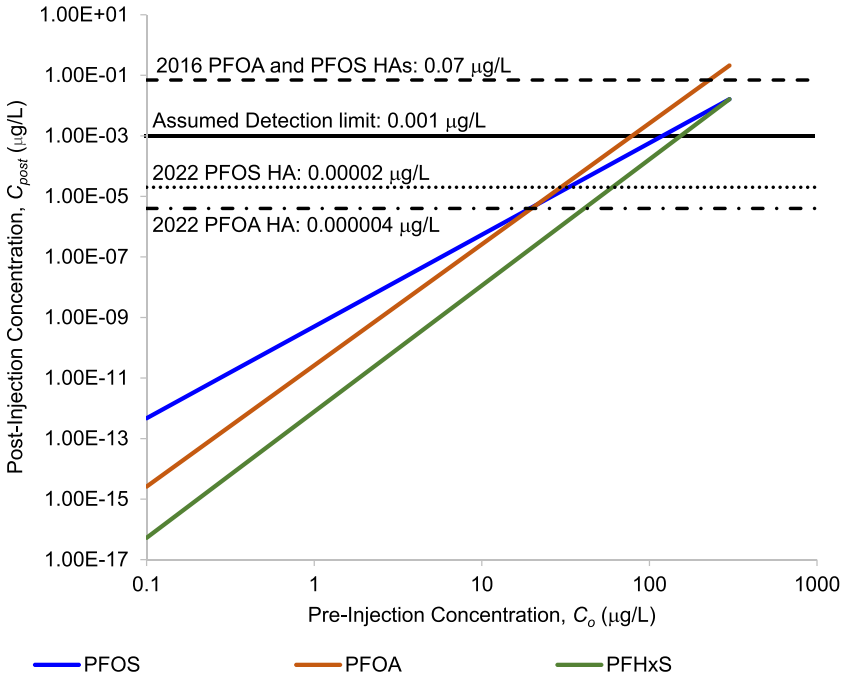

FIGURE 8 Re-equilibrated PFAS aqueous concentrations immediately following CAC injection (C_{post}), as a function of the preinjection groundwater concentration (C_o). Based on f_{oc} = 0.1%, f_{cac} = 0.1%, K_{oc} = 920 ml/g, ρ_b = 1.6 g/ml, and the following Freundlich isotherm parameters for PFOS: K_f = 12,000, a = 0.33; PFOA: K_f = 580, a = 0.25; and PFHxS: K_f = 1240, a = 0.24. K_f units are in mg/kg (mg/L)$^{-a}$. CAC, colloidal activated carbon; HA, health advisories; PFAS, per- and polyfluoroalkyl substances; PFHxS, perfluorohexanesulfonic acid; PFOA, perfluorooctanoic acid; PFOS, perfluorooctanesulfonic acid.

process. The model simulates the linear sorption isotherm for the organic carbon fraction outside of the CAC zone (and in this zone before CAC injection), and the Freundlich sorption isotherm for CAC is modeled inside the CAC zone after injection.

The postinjection aqueous concentration immediately after CAC injection (C_{post}) is calculated in the model in units of mg/L using (Carey et al., 2019)

$$C_{post} = \left[\frac{C_o(\theta + K_{oc} f_{oc} \rho_b)}{K_f f_{cac} \rho_b}\right]^{1/a}, \quad (5)$$

where C_o is the preinjection PFAS concentration (mg/L), K_{oc} is the organic carbon partitioning coefficient (L/g), and f_{oc} is the fraction of organic carbon content (g/g).

Figure 8 shows the calculated C_{post} for C_o ranging from 0.1 to 1000 μg/L, for the three PFAS of interest that were considered in the model analysis: PFOS, PFOA, and PFHxS. The Freundlich isotherm parameters (K_f and a) discussed earlier for the AFFF-impacted groundwater sample were used in Equation (5) to generate Figure 8. f_{oc} was assumed to be 0.1%, ρ_b is 1.6 g/ml, θ is 0.2 m^3/m^3, and f_{cac} is 0.08% based on the middle of the range observed by McGregor (2018), McGregor (2020a), McGregor and Benevenuto (2021), and McGregor and Zhao (2021).

Figure 8 shows that C_{post} exceeds the federal HAs for PFOS and PFOA when C_o is 27 and 15 μg/L, respectively. C_{post} exceeds an example detection limit of 0.001 μg/L when C_o for PFOS, PFOA, and PFHxS is 100, 60, and 140 μg/L, respectively. The median state-wide criterion of 0.07 μg/L is only exceeded at even higher plume

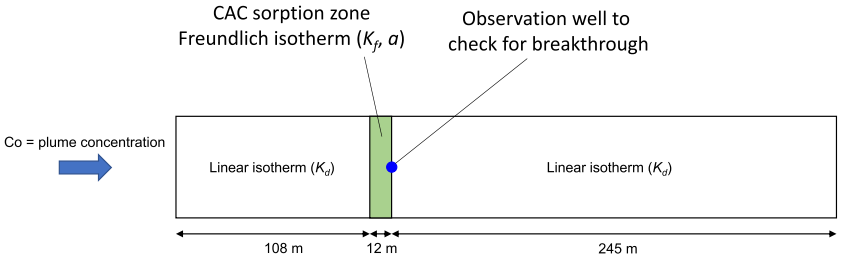

FIGURE 9 One-dimensional model domain extent and features. CAC, colloidal activated carbon.

concentrations. These results indicate that if a detection limit of 0.001 µg/L or higher is used as the remediation criteria, then postinjection concentrations for these three PFAS of interest will be below detection limits immediately after CAC injection for many of the sites in the AFFF-impacted airport sites database, based on a review of Figure 1.

To assess the range in CAC longevity under varying site conditions, a one-dimensional groundwater flow and reactive transport model was developed using MODFLOW and ISR-MT3DMS (Porewater Solutions, 2022). The one-dimensional domain is shown in Figure 9. The model domain has a length of 365 m parallel to groundwater flow, 1 m wide, and a saturated thickness of 3 m. Grid spacing varied from a minimum of 0.25 m within and adjacent to the CAC sorption zone, up to 5 m at the upgradient and downgradient portions of the model domain. There are 282 columns in the one-dimensional model. An observation well was incorporated in the model at the downgradient CAC boundary, to facilitate the assessment of when PFAS breakthrough occurred (based on when applicable criteria were first exceeded at this observation well location).

Fixed-head boundary conditions were defined in MODFLOW to create a horizontal hydraulic gradient of 0.003 m/m. Infiltration was not simulated. The base case hydraulic conductivity was 3.05 m/day, which corresponds to an average linear groundwater velocity of about 17 m/year, which is around the average groundwater velocity observed at contaminated sites based on data cited in Seyedabbasi et al. (2010).

For the longevity analysis, it was assumed that CAC would be injected into a downgradient plume at an AFFF-impacted airport site. This type of site will likely have high precursor and organic co-contaminant concentrations in source zones which may competitively inhibit the adsorption of the PFAS of interest. Therefore, it is recommended that CAC sorption zones be implemented some distance downgradient of source zones at this type of site, where precursors are more likely to have been filtered out of the PFAS plume via sorption, and organic co-contaminants may have already been remediated. PFAS plume concentrations upgradient of the CAC zone were assumed to be approximately three times lower than the maximum PFAS concentrations observed at AFFF-impacted airport sites, which may represent a conservative overestimate of plume concentrations.

The base case simulation included three solutes: PFOS, PFHxS, and PFOA. As shown in Figure 9, the CAC zone was modeled to be 12 m in length, starting at a distance of 108 m downgradient from the model influent boundary to ensure that it is sufficiently far from the fixed-concentration boundary. (The actual distance of 108 m does not have special meaning, this is simply related to when the minimum grid spacing was at 0.25 m in the model domain.) The CAC injection time was specified in ISR-MT3DMS to be 1000 days after the start of the simulation, and the upgradient model boundary was specified to have a fixed concentration representative of a PFAS plume (12 µ/L for PFOS, 7 µg/L for PFHxS, and 2 µg/L for PFOA), which is equivalent to three times lower than the median site maximum (source) concentrations shown in Figure 1. The initial concentrations for each solute were defined to be the same as the upgradient fixed concentration so that the plume started at steady-state conditions in the model simulation.

Table 2 describes the flow and transport model input parameters specified for the base case scenario (i.e., one-third of median AFFF-impacted airport site concentrations). Sorption parameters are identical to those used to generate the C_{post} versus C_o chart in Figure 8. These model simulations implicitly account for some competitive sorption effects because the Freundlich isotherms are based on a groundwater sample (i.e., mixture) that includes elevated PFAS concentrations and relatively high organic matter (DOC of 23.8 cc mg/L).

Table 3 presents the simulated CAC longevity for PFOS, PFOA, and PFHxS based on which regulatory or guidance values are used to define breakthrough: federal HAs (PFOS and PFOA only), a typical detection limit of 0.001 µg/L, and the median state-specific criterion of 0.07 µg/L for all three PFAS of interest. Model results show that there is only a 1.5% difference in simulated longevity between the minimum and maximum criteria even though the breakthrough concentrations vary by orders of magnitude. The insensitivity of the longevity for these wide-ranging criteria is due to the sharp breakthrough curves for the CAC sorption zone, as discussed below. This indicates that the modeled PFAS breakthrough curve in the CAC sorption zone is sufficiently sharp that the applicable criterion is unlikely to have a significant influence on CAC remedy longevity. There is uncertainty in what the shape of the breakthrough curve may look like at field sites with significant heterogeneity (e.g., such as in the f_{cac} distribution) and long-term nonideal behavior such as mass transfer limitations.

Table 3 shows that the longevity for PFOS, PFOA, and PFHxS corresponding to a criterion equal to a detection limit of 0.001 µ/L

TABLE 2 Base case model input parameters

Model grid
- No. columns: 282
- Domain length: 365 m
- Minimum grid spacing: 0.25 m
- Maximum grid spacing: 5 m
- Grid width: 1 m
- Saturated thickness: 3.05 m

MODFLOW input parameters
- Upgradient head: 100 m
- Downgradient head: 98.919 m
- Hydraulic conductivity: 3.05 m/day
- Infiltration rate: 0

ISR-MT3DMS input parameters

Upgradient plume concentrations, C_o
- PFOS: 12 μg/L
- PFHxS: 7 μg/L
- PFOA: 2 μg/L

Default time step: 1 day
Effective porosity: 0.2
Soil dry bulk density: 1.6 g/ml
Longitudinal dispersivity: 3.0 m
Fraction of organic carbon, f_{oc}: 0.1%
Organic carbon partitioning coefficient, K_{oc}
- PFOS: 920 ml/g
- PFHxS: 130 ml/g
- PFOA: 120 ml/g

Time of CAC injection: 1000 days
CAC zone length: 12 m
Postinjection f_{cac}: 0.08%
Freundlich isotherm parameters in CAC zone
- PFOS: K_f = 12,000 mg/kg (mg/L)$^{-a}$, a = 0.33
- PFHxS: K_f = 1240 mg/kg (mg/L)$^{-a}$, a = 0.24
- PFOA: K_f = 580 mg/kg (mg/L)$^{-a}$, a = 0.25

Abbreviations: CAC, colloidal activated carbon; PFHxS, perfluorohexanesulfonic acid; PFOA, perfluorooctanoic acid; PFOS, perfluorooctanesulfonic acid.

TABLE 3 Simulated CAC longevity based on various criteria

Solute	Longevity (years) based on criteria		
	HA	DL = 0.001 μg/L	State = 0.07 μg/L
PFOS	915	924	936
PFOA	262	265	268
PFHxS	n/a	233	235

Abbreviations: CAC, colloidal activated carbon; DL, detection limit; HA, health advisories;n/a, not available; PFHxS, perfluorohexanesulfonic acid; PFOA, perfluorooctanoic acid; PFOS, perfluorooctanesulfonic acid.

was simulated to be 924, 265, and 233 years, respectively. CAC has the greatest longevity for PFOS, even though PFOS is present at higher concentrations than the other species because the sorption affinity for PFOS is considerably higher than PFOA and PFHxS. There was only a 15% difference in CAC longevity for PFOA and PFHxS, so the remainder of the model simulations were conducted based on PFOA because it more frequently has regulatory or guidance values at the federal and state levels. A criterion of 0.001 μg/L (typical detection limit) was used to calculate longevity for the remaining simulations because the federal HA is too low to be attainable in practice given that it falls below typical detection limits for PFOA and PFOS.

Two additional simulations were conducted to determine how reductions in the fraction of CAC in soil (f_{cac}) from 0.08% (base case) to 0.02% and 0.04% would affect longevity. Figure 10 presents the PFOA breakthrough curves at the downgradient CAC sorption zone boundary for these three scenarios. Figure 10 illustrates how sharp the modeled breakthrough curves are, which is why the criteria used do not have a significant influence on the modeled longevity (noted earlier). CAC longevity corresponding to f_{cac} values of 0.02%, 0.04%, and 0.08% was simulated to be 66, 132, and 265 years, respectively. This indicates that longevity is linearly proportional to f_{cac}. Intuitively this makes sense because f_{cac} is a general metric that correlates with the number of available sorption sites on CAC.

Figure 11a–d presents modeled PFOA longevity based on the following changes to the base case scenario:

- Figure 11a: Upgradient plume concentration (C_o) varies from 2 to 50 μg/L;
- Figure 11b: Average linear groundwater velocity varies from 17–245 m/year;
- Figure 11c: K_f varies from 75 to 580 mg/kg (mg/L)$^{-a}$; and
- Figure 11d: a varies from 0.2 to 0.45.

Figure 11a–c indicates that CAC longevity is inversely proportional to C_o and average linear groundwater velocity, and is directly proportional to K_f. This suggests that there may be several options for increasing CAC longevity at a site by incorporating additional components into the final remedial design, such as:

1. Reduce mass flux from a source in the vadose zone, such as paving over a former fire training area to reduce the flux of PFAS of interest from the vadose zone to an underlying aquifer, at least for PFOA and PFHxS.
2. Using pump-and-treat to intercept groundwater in a high-concentration source zone below the water table, and employing CAC at one or more locations in a downgradient plume.
3. Diversion of groundwater flows away from a PFAS source zone below the water table and plume to reduce the groundwater velocity in the plume, either by pumping clean groundwater from the upgradient or possibly the installation of a diversion barrier wall if that proves to be cost-effective.
4. Construct the CAC zone where competitive inhibition from other solutes (e.g., PFAS precursors) is at a minimum, resulting in higher values of K_f.
5. Decrease the hydraulic conductivity of the source zone by soil mixing with clay or other low-permeability materials.

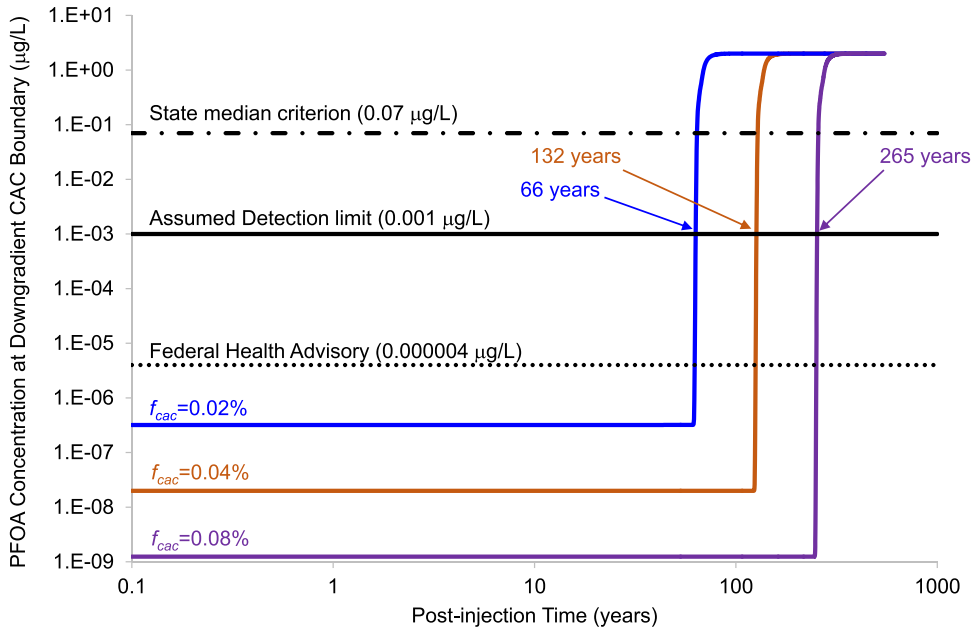

FIGURE 10 Modeled PFOA breakthrough curves at the downgradient boundary of the CAC zone, corresponding to an upgradient plume concentration of 2 µg/L (median at 96 AFFF-impacted airport sites), average linear groundwater velocity of 17 m/year, K_f = 580 (mg/kg)(mg/L)$^{-a}$ and a = 0.25. AFFF, aqueous film-forming foam; CAC, colloidal activated carbon; PFOA, perfluorooctanoic acid.

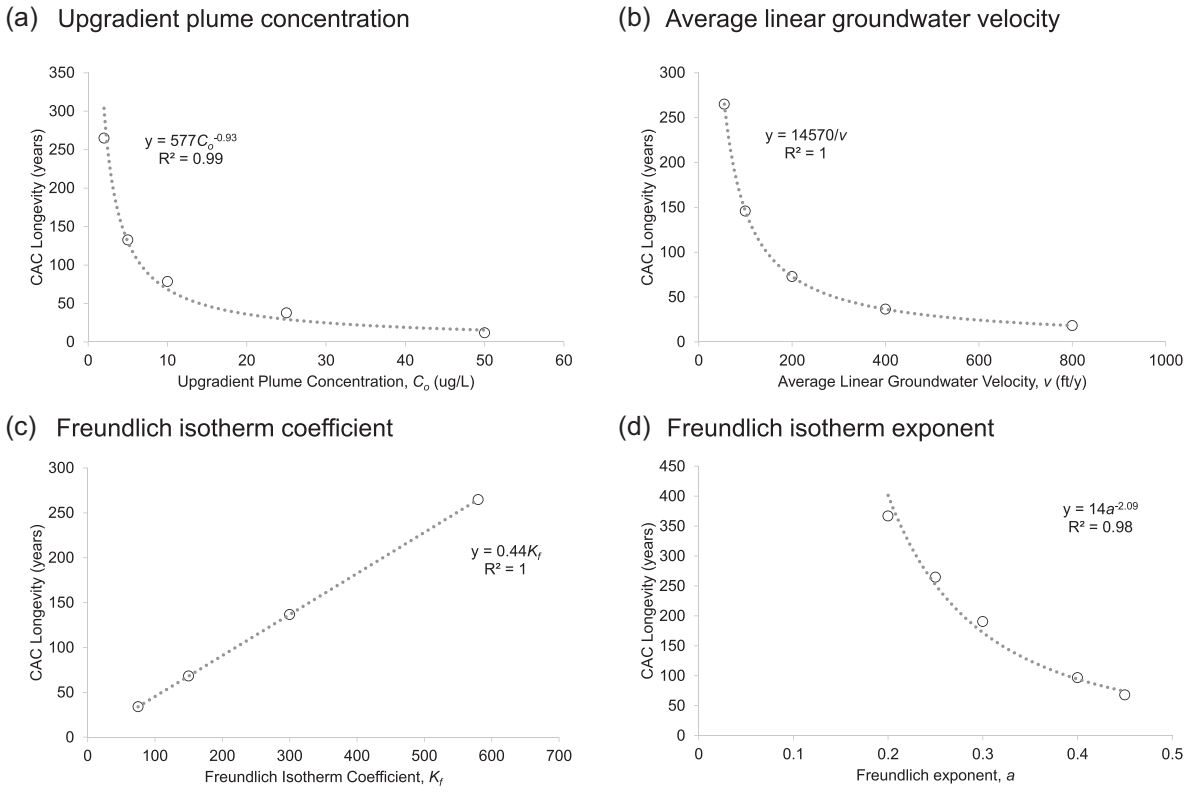

FIGURE 11 Sensitivity of colloidal activated carbon (CAC) Longevity to various site and sorption characteristics. (a) Upgradient plume concentration. (b) Average linear groundwater velocity. (c) Freundlich isotherm coefficient. (d) Freundlich isotherm exponent.

Remedial decisions should also take into account that eventually breakthroughs will occur, resulting in the need for either additional CAC injection or implementation of another remedy. One of the advantages of CAC is that there are currently few viable in situ remedial alternatives for PFAS sites, and CAC implementation may at least limit the further spreading of a plume in the hopes that future technological advancements in PFAS remediation may be realized over the next few decades.

Figure 11d indicates that longevity is also sensitive to the Freundlich (*a*) exponent. This indicates that the Freundlich isotherm parameters will have a significant influence on the modeled CAC longevity. For this reason, it is important to determine site-specific PFAS–CAC isotherms when the modeled longevity has a major influence on remedial decision-making.

8 | CONCLUSION

GAC bench- and full-scale studies indicate that short-chain PFAS exhibit faster breakthrough than the four PFAS of interest defined in this study (PFOS, PFOA, PFHxS, and PFNA), and thus we can expect CAC to have shorter longevity for short-chain PFAAs. Currently, there are only a few states which have regulatory or guidance values for short-chain PFAAs. Consideration should be made regarding potential future regulatory changes (i.e., changes to regulated constituents or clean-up criteria) during the remedial decision-making process.

A review of the SSEHRI database of 1244 sites identified 96 AFFF-impacted militaries and/or civilian airport sites for which maximum PFAS concentrations were provided. Maximum source zone concentrations at these 96 sites had median values of 37, 22, 7, and 0.2 μg/L for PFOS, PFHxS, PFOA, and PFNA. A large proportion (82%) of these sites had total PFOS and PFHxS concentrations that were greater than 70% of the sum of the four PFAS of interest. This is relevant for a CAC adsorption remedy because PFSAs are preferentially adsorbed to activated carbon over PFCAs.

A semiquantitative analysis demonstrates that relative breakthrough times for PFAS in *ex situ* GAC are expected to be substantially faster than for in situ CAC systems. The difference in relative breakthrough times is due to substantial differences in retention times (minutes for GAC vs. months for CAC), and the greater impact of mass transfer limited transport in larger GAC particles.

Field-scale studies of CAC injection at PFAS sites are reviewed, demonstrating that the injection of CAC to facilitate in situ PFAS remediation has been generally successful for both short- and long-chain PFAS in the short-term (0.3–6 years) at most of the 17 field sites, even in the presence of low levels of organic co-contaminants such as chlorinated solvents or petroleum hydrocarbons. The longevity of CAC for in situ PFAS remediation is uncertain and challenging to predict, with only sparse studies available to quantify PFAS adsorption behavior with CAC.

New PFOS, PFHxS, PFOA, and 6:2 FtS isotherms were determined for sorption to CAC for a groundwater sample from an AFFF-impacted site. Freundlich isotherms in this current study were estimated for PFOS (K_f = 12,000 mg/kg [mg/L]$^{-a}$ and a = 0.33), PFHxS (K_f = 1240 mg/kg [mg/L]$^{-a}$ and a = 0.24), PFOA (K_f = 580 mg/kg [mg/L]$^{-a}$ and a = 0.25), and 6:2 FtS (K_f = 3900 mg/kg [mg/L]$^{-a}$ and a = 0.2). DOC was relatively high in the groundwater sample (23.8 mg/L), and likely played a role in reducing the sorption of PFAS to CAC during the batch tests. Development of site-specific PFAS isotherms for CAC based on one or more groundwater samples with representative DOC, geochemistry, and co-contaminants will account for important competitive sorption behavior, resulting in more representative model predictions of CAC remedy longevity.

Numerical modeling was conducted to assess the sensitivity of CAC longevity to various site and remedial design characteristics. The modeled longevity for PFAS was shown to be insensitive to clean-up criteria which varied by up to 4 orders of magnitude, because of the sharp PFAS breakthrough curves modeled to occur in CAC zones. Longevity is inversely proportional to upgradient plume concentration and velocity and is directly proportional to K_f. Longevity is sensitive to small changes in the Freundlich exponent (*a*) due to the nonlinear behavior of PFAS adsorption to activated carbon, including CAC. Smaller values of *a* result in greater remedy longevity for the scenarios considered in this model analysis. Remedial alternatives such as paving the surface in former fire training areas to reduce the mass flux from the unsaturated zone, or diverting clean water flow (if applicable) around the downgradient PFAS plume will increase the longevity of a CAC remedy at PFAS sites.

ACKNOWLEDGMENTS

The authors would like to thank REGENESIS for providing the colloidal activated carbon field study information presented in Table 1b. They would also like to thank Dr. Charles Schaefer for providing us with the groundwater sample from an aqueous film-forming foam-impacted site. At last, they would like to acknowledge the detailed and thoughtful comments by anonymous reviewers which helped to improve this manuscript. This study was supported by the Natural Sciences and Engineering Research Council of Canada Alliance Program and by Porewater Solutions.

REFERENCES

Agency for Toxic Substances and Disease Registry (ATSDR). (2018). PFAs toxicological profile key messages, centers for disease control and prevention, June 2018. https://stacks.cdc.gov/view/cdc/84237

Appleman, T. D., Higgins, C. P., Quiñones, O., Vanderford, B. J., Kolstad, C., Zeigler- Holady, J. C., & Dickenson, E. R. V. (2014). Treatment of poly- and perfluoroalkyl substances in U.S. full-scale water treatment systems. *Water Research*, *51*, 246–255.

Bakkaloglu, S., Ersan, M., Karanfil, T., & Apul, O. G. (2021). Effect of superfine pulverization of powdered activated carbon on adsorption of carbamazepine in natural source waters. *Science of the Total Environment*, *793*, 148473.

Belkouteb, N., Franke, V., McCleaf, P., Köhler, S., & Ahrens, L. (2020). Removal of per- and polyfluoroalkyl substances (PFASs) in a full-scale drinking water treatment plant: Long-term performance of granular activated carbon (GAC) and influence of flow-rate. *Water Research*, *182*, 115913.

Cantoni, B., Turolla, A., Wellmitz, J., Ruhl, A. S., & Antonelli, M. (2021). Perfluoroalkyl substances (PFAS) adsorption in drinking water by granular activated carbon: Influence of activated carbon and PFAS characteristics. *Science of the Total Environment*, *795*, 148821.

Carey, G. R., McGregor, R., Pham, A. L.-T., Sleep, B., & Hakimabadi, S. G. (2019). Evaluating the longevity of a PFAS in situ colloidal activated carbon remedy. *Remediation Journal*, *29*, 17–31.

Chularueangaksorn, P., Tanaka, S., Fujii, S., & Kunacheva, C. (2014). Batch and column adsorption of perfluorooctane sulfonate on anion exchange resins and granular activated carbon. *Journal of Applied Polymer Science*, *131*, 39782.

Du, Z., Deng, S., Bei, Y., Huang, Q., Wang, B., Huang, J., & Yu, G. (2014). Adsorption behavior and mechanism of perfluorinated compounds on various adsorbents—A review. *Journal of Hazardous Materials*, *274*, 443–454.

Englund, S. (2015). *Evaluation of the removal efficiency of perfluoroalkyl substances in drinking water* (Masters thesis). Uppsala University. 2015.

Environmental Protection Agency (EPA) (2022). *Drinking water health advisories for PFAS fact sheet for communities* [Fact Sheet].

Franke, V., Belkouteb, N., McCleaf, P., Kohler, S. J., & Ahrens, L. (2017). Evaluation of the removal efficiency of PFASs in a full-scale drinking water treatment plant [Conference presentation]. Swedish University of Agricultural Sciences.

Hansen, M. C., Børresen, M. H., Schlabach, M., & Cornelissen, G. (2010). Sorption of perfluorinated compounds from contaminated water to activated carbon. *Journal of Soils and Sediments*, *10*, 179–185.

Interstate Technology and Regulatory Council (ITRC) (2020). *Regulation of per- and polyfluoroalkyl substances (PFAS)* [Fact sheet].

Lindegren, K. (2015). *Evaluation of the removal efficiency of per- and polyfluoroalkyl substances in drinking water using nanofiltration membranes, active carbon and anion exchange* (Masters thesis). Uppsala University.

Liu, C., Hatton, J., Arnold, W. A., Simcik, M. F., & Pennell, K. D. (2020). In situ sequestration of perfluoroalkyl substances using polymer-stabilized powdered activated carbon. *Environmental Science & Technology*, *54*, 6929–6936.

McCleaf, P., Englund, S., Östlund, A., Lindegren, K., Wiberg, K., & Ahrens, L. (2017). Removal efficiency of multiple poly- and perfluoroalkyl substances (PFASs) in drinking water using granular activated carbon (GAC) and anion exchange (AE) column tests. *Water Research*, *120*, 77–87.

McGregor, R. (2018). In situ treatment of PFAS-impacted groundwater using colloidal activated carbon. *Remediation Journal*, *28*, 33–41.

McGregor, R. (2020a). Six pilot-scale studies evaluating the in situ treatment of PFAS in groundwater. *Remediation*, *30*, 39–50.

McGregor, R. (2020b). Distribution of colloidal and powdered activated carbon for the in situ treatment of groundwater. *Journal of Water Resource and Protection*, *12*, 1001–1018.

McGregor, R., & Benevenuto, L. (2021). The effect of heterogeneity on the distribution and treatment of PFAS in a complex geologic environment. *Frontiers in Environmental Chemistry*, *2*, 729779.

McGregor, R., & Zhao, Y. (2021). The in situ treatment of TCE and PFAS in groundwater within a silty sand aquifer. *Remediation Journal*, *31*, 7–17.

Murray, C. C., Vatankhah, H., McDonough, C. A., Nickerson, A., Hedtke, T. T., Cath, T. Y., Higgins, C. P., & Bellona, C. L. (2019). Removal of per- and polyfluoroalkyl substances using super-fine powder activated carbon and ceramic membrane filtration. *Journal of Hazardous Materials*, *366*, 160–168.

Ochoa-Herrera, V., & Sierra-Alvarez, R. (2008). Removal of perfluorinated surfactants by sorption onto granular activated carbon, zeolite and sludge. *Chemosphere*, *72*, 1588–1593.

Ostlund, A. (2015). *Removal efficiency of perfluoroalkyl substances (PFASs) in drinking water* (Masters thesis). Uppsala University.

Park, M., Wu, S., Lopez, I. J., Chang, J. Y., Karanfil T., & Snyder, S. A. (2020). Adsorption of perfluoroalkyl substances (PFAS) in groundwater by granular activated carbons: Roles of hydrophobicity of PFAS and carbon characteristics. *Water Research*, *170*, 115364.

Porewater Solutions. (2022). ISR-MT3DMS users guide for simulating multispecies reactive transport.

Qu, Y., Zhang, C., Li, F., Bo, X., Liu, G., & Zhou, Q. (2009). Equilibrium and kinetics study on the adsorption of perfluorooctanoic acid from aqueous solution onto powdered activated carbon. *Journal of Hazardous Materials*, *169*, 146–152.

REGENESIS. (2022). PFAS removed from aquifer at hazardous waste site where AFFF was used—Case study: Results demonstrate 99.9% reduction of high concentrations of PFOS and PFOA. https://regenesis.com/wp-content/uploads/2019/12/TetraTech-Co-Branded-Case-Study-PFAS-Ridge-Run.pdf

Seyedabbasi, M. A., Newell, C. J., Adamson, D. T., & Sale, T. C. (2010). Relative contribution of DNAPL dissolution and matrix diffusion to the long-term persistence of chlorinated solvent source zones. *Journal of Contaminant Hydrology*, *134–135*, 69–81.

Siriwardena, D. P., Crimi, M., Holsen, T. M., Bellona, C., Divine, C., & Dickenson, E. (2019). Influence of groundwater conditions and co-contaminants on sorption of perfluoroalkyl compounds on granular activated carbon. *Remediation Journal*, *29*, 5–15.

Xiao, X., Ulrich, B. A., Chen, B., & Higgins, C. P. (2017). Sorption of poly- and perfluoroalkyl substances (PFASs) relevant to aqueous film-forming foam (AFFF)-impacted groundwater by biochars and activated carbon. *Environmental Science & Technology*, *51*, 6342–6351.

Yu, J., & Hu, J. (2011). Adsorption of perfluorinated compounds onto activated carbon and activated sludge. *Journal of Environmental Engineering*, *137*(10), 945–951.

Yu, Q., Zhang, R., Deng, S., Huang, J., & Yu, G. (2009). Sorption of perfluorooctane sulfonate and perfluorooctanoate on activated carbons and resin: Kinetic and isotherm study. *Water Research*, *43*, 1150–1158.

Zhang, D., He, Q., Wang, M., Zhang, W., & Liang, Y. (2021). Sorption of perfluoroalkylated substances (PFASs) onto granular activated carbon and biochar. *Environmental Technology*, *42*(12), 1798–1809.

Zhang, D., Luo, Q., Gao, B., Chiang, S.-Y. D., Woodward, D., & Huang, Q. (2016). Sorption of perfluorooctanoic acid, perfluorooctane sulfonate and perfluoroheptanoic acid on granular activated carbon. *Chemosphere*, *144*, 2336–2342.

Zhi, Y., & Liu, J. (2015). Adsorption of perfluoroalkyl acids by carbonaceous adsorbents: Effect of carbon surface chemistry. *Environmental Pollution*, *202*, 168–176.

AUTHOR BIOGRAPHIES

Grant R. Carey, PhD, PEng, is the president of Porewater Solutions in Ottawa, ON, Canada. Dr. Carey specializes in per- and polyfluoroalkyl substances (PFAS) environmental forensics, litigation, groundwater modeling, nonaqueous-phase liquid remediation, and back diffusion. Dr. Carey is recognized for his development of innovative modeling and visualization tools and is currently collaborating with various universities on PFAS remediation research. He received a BASc degree from the University of Waterloo, an MEng degree from Carleton University, and a PhD degree from the University of Guelph. He is an adjunct research professor in environmental engineering at Carleton University.

Seyfollah G. Hakimabadi, MS, is a PhD candidate in the Department of Civil and Environmental Engineering at the University of Waterloo. He received a BS degree in chemical engineering from the Amirkabir University of Technology, and an MS degree in chemical engineering from the Ferdowsi University of Mashhad, Iran.

Mantake Singh, BEng, is a MASc candidate in environmental engineering in the Department of Civil and Environmental Engineering at Carleton University. He received a BEng degree in civil engineering at the College of Technology and Engineering in Udaipur, India.

Rick McGregor, MSc, MBA, is a hydrogeologist with InSitu Remediation Services Ltd., based in Canada. Mr. McGregor has a BSc degree in geology and an MSc degree in hydrogeology and geochemistry from the University of Waterloo along with an MBA degree from Wilfrid Laurier University. He has over 27 years of experience in research, consulting, and contracting. His current focus is on the remediation of impacted groundwater

Claire Woodfield, BASc, is a junior environmental consultant. She received her BASc degree in environmental engineering from Carleton University.

Paul J. Van Geel, PhD, is a professor of environmental engineering at Carleton University and specializes in hydrogeology and solid waste management, flow and transport in the saturated and unsaturated zones, impacts of real-world soil/nonaqueous-phase liquid (NAPL) wettability on migration, distribution, and remediation of NAPL-contaminated sites. Dr. Van Geel received his BASc and PhD degrees from the University of Waterloo.

Anh Le-Tuan Pham, PhD, is an assistant professor of civil and environmental engineering at the University of Waterloo. His research group investigates contaminant fate and transformation. The current research focuses on developing novel technologies for the remediation of contaminated soil and groundwater, treatment of oil sands process water, and removal of emerging contaminants. He received his BS degree in chemical engineering from the Hanoi University of Technology, and MS and PhD degrees in civil and environmental engineering from the University of California, Berkeley.

SUPPORTING INFORMATION

Additional supporting information can be found online in the Supporting Information section at the end of this article.

How to cite this article: Carey, G. R., Hakimabadi, S. G., Singh, M., McGregor, R., Woodfield, C., Van Geel, P. J., & Pham, A.-T. (2022). Longevity of colloidal activated carbon for in situ PFAS remediation at AFFF-contaminated airport sites. *Remediation*, 33, 3–23. https://doi.org/10.1002/rem.21741